Allergy Asthma Immunol Res. 2024 Jul;16(4):e33
https://doi.org/10.4168/aair.2024.16.e33
pISSN 2092-7355·eISSN 2092-7363

Allergy, Asthma & Immunology Research AAIR

Original Article

Check for updates

TNFSF11/TNFRSF11A Axis Amplifies HDM-Induced Airway Remodeling by Strengthening TGFβ1/STAT3 Action

Dong Zhang [1†], **Jintao Zhang** [2†], **Qian Qi** [2], **Yun Pan** [1], **Rong Zeng** [1], **Changjuan Xu** [2], **Xiaofei Liu** [2], **Jiawei Xu** [2], **Mingxia Gao** [2], **Tingting Gao** [2], **Jian Zhang** [2], **Shuochuan Shi** [2], **Liang Dong** [1,2*]

[1]Department of Respiratory, Shandong Provincial Qianfoshan Hospital, Shandong University, Jinan, China
[2]Department of Respiratory and Critical Care Medicine, The First Affiliated Hospital of Shandong First Medical University and Shandong Provincial Qianfoshan Hospital, Shandong Institute of Respiratory Diseases, Jinan, China

OPEN ACCESS

Received: Jan 23, 2024
Revised: Apr 27, 2024
Accepted: May 17, 2024
Published online: Jun 27, 2024

Correspondence to
Liang Dong, MD, PhD
Department of Respiratory, Shandong Provincial Qianfoshan Hospital, Shandong University; Department of Respiratory and Critical Care Medicine, The First Affiliated Hospital of Shandong First Medical University and Shandong Provincial Qianfoshan Hospital, Shandong Institute of Respiratory Diseases, No. 16766 Jingshi Road, Jinan 250014, Shandong, China.
Tel: +86-13505401207
Fax: +18653182166931
Email: dl5506@126.com

†The authors contributed mainly to this study.

Copyright © 2024 The Korean Academy of Asthma, Allergy and Clinical Immunology · The Korean Academy of Pediatric Allergy and Respiratory Disease
This is an Open Access article distributed under the terms of the Creative Commons Attribution Non-Commercial License (https://creativecommons.org/licenses/by-nc/4.0/) which permits unrestricted non-commercial use, distribution, and reproduction in any medium, provided the original work is properly cited.

ORCID iDs
Dong Zhang
https://orcid.org/0000-0001-7323-7699
Jintao Zhang
https://orcid.org/0000-0002-1309-6836

ABSTRACT

Purpose: Asthma, an airway inflammatory disease, involves multiple tumor necrosis factors (TNF). TNF ligand superfamily member 11 (TNFSF11) and its known receptor, TNF receptor superfamily 11A (TNFRSF11A), has been implicated in asthma; however, the related mechanisms remain unknown.
Methods: The serum and bronchial airway of patients with asthma and healthy subjects were examined. The air-liquid interface of primary human bronchial epithelial (HBE) cells, and *Tnfsf11*$^{+/-}$ mouse, *Tnfrsf11a*$^{+/-}$ mouse, and a humanized HSC-NOG-EXL mouse model were established. This study constructed short hairpin RNA (shRNA) of *TNFSF11*, *TNFRSF11A*, transforming growth factor β1 (*TGFβ1*), and transforming growth factor β receptor type 1 (*TGFβR1*) using lentivirus to further examine the ability of TNFSF11 protein.
Results: This study was the first to uncover TNFSF11 overexpression in the airway and serum of asthmatic human subjects, and the TNFSF11 in serum was closely correlated with lung function. The TNFSF11/TNFRSF11A axis deficiency in *Tnfsf11*$^{+/-}$ or *Tnfrsf11a*$^{+/-}$ mice remarkably attenuated the house dust mite (HDM)-induced signal transducer and activator of transcription 3 (STAT3) action and remodeling protein expression. Similarly, the HDM-induced STAT3 action and remodeling protein expression in HBE cells decreased after pretreatment with *TNFSF11* or *TNFRSF11A* shRNA. Meanwhile, the expression of the remodeling proteins induced by TNFSF11 significantly decreased after pretreatment with-stattic (inhibitor of STAT3 phosphorylation) in HBE cells. The STAT3 phosphorylation and remodeling protein expression induced by TNFSF11 obviously decreased after pretreatment with *TGFβ1* or *TGFβR1* shRNA in HBE cells. The above results also verified that blocking TNFSF11 with denosumab alleviated airway remodeling via the TGFβ1/STAT3 signaling in the humanized HSC-NOG-EXL mice with HDM-induced asthma.
Conclusions: TGFβ1/STAT3 action was closely correlated with TNFSF11/TNFRSF11A axis-mediated airway remodeling. This study presented a novel strategy that blocks the TNFSF11/TNFRSF11A axis to exert a protective effect against asthma.

Keywords: TNFSF11; TNFRSF11A; HDM; airway remodeling

Provisional

Generated by ⁄miinkpress

Allergy, Asthma & Immunology Research AAIR

Qian Qi
https://orcid.org/0000-0002-5813-3194
Yun Pan
https://orcid.org/0000-0002-5014-0322
Rong Zeng
https://orcid.org/0000-0003-1320-8815
Changjuan Xu
https://orcid.org/0000-0001-8414-2986
Xiaofei Liu
https://orcid.org/0000-0002-7285-7578
Jiawei Xu
https://orcid.org/0000-0002-6289-5589
Mingxia Gao
https://orcid.org/0000-0001-7546-5863
Tingting Gao
https://orcid.org/0009-0006-0145-329X
Jian Zhang
https://orcid.org/0000-0001-8391-7161
Shuochuan Shi
https://orcid.org/0009-0000-4648-4125
Liang Dong
https://orcid.org/0000-0001-7707-9982

Disclosure
There are no financial or other issues that might lead to conflict of interest.

Provisional
Provisional

INTRODUCTION

Asthma is characterized by excessive mucus secretion and limited expiratory airflow and affects approximately 4% of the world population, imposing a serious medical burden.[1] This condition is complicated in many aspects, including personal constitution and external environment; and house dust mite (HDM) is the main allergen in indoor air.[2] The airway epithelium forms a tight barrier and serves as the first line of defense against pathogens. Long-term exposure to allergens changes the epithelial structure and contributes to airway mucus hypersecretion and remodeling.[3] One of the causes of death in patients with severe asthma is pulmonary airway obstruction caused by mucus hypersecretion. Therefore, an in-depth study of the pathogenesis of airway epithelia could aid in improving the living conditions of patients with asthma.

The occurrence and development of asthma are closely related to the tumor necrosis factor (TNF) family.[4] TNF ligand superfamily member 11 (TNFSF11, also known as RANKL) is a type II transmembrane protein ligand that binds to type I transmembrane protein receptor of TNF receptor superfamily 11A (TNFRSF11A, also known as RANK) and activates inflammatory pathways, triggering the signal cascade.[5] TNF receptor superfamily 11B (TNFRSF11B, also known as OPG) is a decoy receptor that inhibits the interaction between TNFSF11 and TNFRSF11A by binding to TNFSF11; it has high affinity and effectively interferes with the activation of downstream signals.[6] TNFSF11/TNFRSF11A plays a major role in bone metabolic diseases.[7] Xiong et al.[8] demonstrated that TNFSF11 is involved in muscle atrophy and dysfunction in smoking-induced chronic obstructive pulmonary disease. Gregorczyk et al.[9,10] and Yang et al.[11] showed that blocking TNFSF11/TNFRSF11A with TNFRSF11B is a therapeutic strategy for asthma. Transforming growth factor β1 (TGFβ1)/signal transducer and activator of transcription 3 (STAT3) signaling plays an important role in asthma progression.[12] However, the mechanisms underlying the relation between the TNFSF11/TNFRSF11A axis and airway remodeling remain unknown.

Here, we confirmed the effects of TNFSF11 on asthma using human serum and airway samples. Human bronchial epithelial (HBE) cells pretreated with *TNFSF11* short hairpin RNA (shRNA) or *TNFRSF11A* shRNA and *Tnfsf11*$^{+/-}$ and *Tnfrsf11a*$^{+/-}$ mice were used to verify the effect of TNFSF11/TNFRSF11A on HDM-induced asthma. Messenger RNA transcriptomics showed the underlying mechanism of TGFβ1/STAT3 signaling, which was confirmed by pretreating HBE cells with STAT3 phosphorylation inhibitor, *TGFβ1* or transforming growth factor β receptor type 1 (*TGFβR1*) shRNA. A humanized HSC-NOG-EXL mouse model was constructed to validate the molecular mechanisms in a near-clinical manner after treatment with denosumab (anti-human TNFSF11).

MATERIALS AND METHODS

Reagents

HDM was obtained from Greer Laboratories (Lenoir, NC, USA). Denosumab was purchased from Selleck (Shanghai, China), and 4,6-diamino-2-phenylindole dihydrochloride (DAPI, 28718-90-3) was acquired from Sigma-Aldrich (St. Louis, MO, USA). Anti-vimentin (ET1610-39), anti-fibronectin (ET1702-25), anti-N-cadherin (ET1607-37), anti-EPCAM (EM1111), anti-glyceraldehyde 3-phosphate dehydrogenase (GAPDH) (ET1601-4), anti-TGFβ1 (ER31210), anti-TGFβR1 (ER1917-65), anti-interleukin (IL)-4 (ER1706-55), anti-IL-5 (HA500081),

https://doi.org/10.4168/aair.2024.16.e33

horseradish peroxidase (HRP)-conjugated goat anti-mouse immunoglobulin (Ig)G (HA1006), and HRP-conjugated goat anti-rabbit IgG (HA1001) were obtained from HUABIO (Zhejiang, China). Anti-collagen I (ab260043), anti-STAT3 (ab68153), anti-p-STAT3 (ab76315), anti-p-STAT5 (ab32364), anti-p-STAT6 (ab32520), and anti-p-JAK2 (ab32101) were purchased from Abcam (Cambridge, UK). Recombinant human TNFSF11 protein (rhTNFSF11, AF-310-01) was obtained from Thermo Fisher Scientific (Waltham, MA, USA). Recombinant mouse TNFSF11 protein (rmTNFSF11, 462-TEC) was provided from RD-Biotech (Franche-Comte, France). Bicinchoninic acid (BCA) protein assay (PC0020), hematoxylin–eosin (HE) staining (G1120), periodic acid–Schiff (PAS) staining (G1280), Masson staining (G1346), enzyme-linked immunosorbent assay (ELISA) IL-4 (SEKM-0005), ELISA IL-33 (SEKM-0028), and broad-spectrum SP (SP0041) kits were bought from Solarbio (Beijing, China). Anti-TNFSF11 (sc-52950), anti-eosinophil major basic protein (EMBP, sc-365701), and anti-TNFRSF11A (sc-374360) were obtained from Santa Cruz Biotechnology (Dallas, TX, US). Lentiviruses of human *TNFSF11* shRNA (sc-29464-V), human *TNFRSF11A* shRNA (sc-42960-V), human *TGFβ1* shRNA (sc-270322-V), and human *TGFβR1* shRNA (sc-40222-V) were purchased from Santa Cruz Biotechnology. Dylight 488 goat anti-mouse IgG (A23210), Dylight 488 goat anti-rabbit IgG (A23220), and Dylight 549 goat anti-rabbit IgG (A23320) were sourced from Abbkine (Wuhan, China). CY5 goat anti-mouse IgG (GB27301) was obtained from Servicebio (Wuhan, China). ELISA kits for human TNFSF11 (EK0842) and mouse TNFSF11 (EK0843) were provided by Boster (Wuhan, China).

Human sample collection

The criteria for asthma diagnosis were based on the 2021 Global Strategy for Asthma Management and Prevention.[13] Serum samples were collected from the respiratory outpatient department and physical examination center of the First Affiliated Hospital of Shandong First Medical University. Lung specimens were collected from patients with asthma and patients with suspected tumors who were finally diagnosed as normal using the respiratory endoscope of the First Affiliated Hospital of Shandong First Medical University. The clinical characteristics of the patients are shown in **Supplementary Table S1**. This study was approved by the Human Ethics Review Committee (S132) of the First Affiliated Hospital of Shandong First Medical University.

Inflammation-related biomarkers

The Olink inflammatory biomarker panel was used to analyze inflammatory markers in serum from patients with asthma (n = 11) and normal patients (n = 10).[14] The panel requires only 1 μL of serum to simultaneously analyze 92 different inflammatory factors. Those 92 different target proteins were bound by a pair of oligonucleotide-labeled antibody probes, which were close to one another, and the oligonucleotides hybridized in pairs. This process resulted in unique polymerase chain reaction (PCR) target sequences under DNA polymerase action. The target sequences were obtained using microfluidic real-time PCR. Data were expressed as normalized protein expression (NPX) after quality control and log2 normalization. The median value corresponded to protein expression.

Bioinformatics analysis

t-test was performed between two groups, and $P < 0.05$ indicated that a screened protein meets the threshold for Olink data and is a differentially expressed protein (DEP). A differential protein heatmap was used for clustering analysis based on the similarity of protein expression profiles in serum. A volcano plot was employed to visualize DEP distribution. The DEPs were then subjected to Gene Ontology (GO) and Kyoto Encyclopedia

Provisional Provisional

Allergy, Asthma & Immunology Research AAIR

of Genes and Genomes (KEGG) functional analyses. Finally, the STRING protein-protein interaction (PPI) was employed for interaction analysis on the identified proteins. Bioinformatics analysis was completed by LC-Bio Technologies Co., Ltd. (Hangzhou, China).

Animal grouping and treatment

The animal study was approved by the Animal Ethics Review Committee (S131) of the First Affiliated Hospital of Shandong First Medical University. The animal operation conformed to the Guidelines for the Care and Use of Experimental Animals of the National Institute of Health.

Female C57BL/6 mice were purchased from Jinan Pengyue Animal Feeding Co., Ltd. (Jinan, China). The mice (n = 6, 7–8 weeks, 18–20 g) were stimulated by HDM or rmTNFSF11.

Tnfsf11 is located on chromosome 14, and *Tnfrsf11a* is located on chromosome 1 in mice. An sgRNA was designed using CRISPR/Cas9 technology for the high-throughput electrotransfer of fertilized eggs to obtain mice with *Tnfsf11* and *Tnfrsf11a* genes. However, $Tnfsf11^{-/-}$ or $Tnfrsf11a^{-/-}$ caused the death of mice. Thus, $Tnfsf11^{+/-}$ and $Tnfrsf11a^{+/-}$ mice were sourced from Saiye Biology for experimental studies. The gene identification report of $Tnfsf11^{+/-}$ and $Tnfrsf11a^{+/-}$ mice can be found in **Supplementary Fig. S1**.

NOG-EXL mice are transgenic mouse models constructed by transferring human cytokine granulocyte-macrophage colony-stimulating factor (GM-CSF) and IL-3 on the basis of NOG. NOG-EXL mice transplanted with human cord blood-derived hematopoietic stem cells (HuCD34+huHSC) nearly emulate the human immune system including mature granulocytes, dendritic cells, mast cells, monocytes, macrophages, B cells, and T cells.[15] Humanized HSC-NOG-EXL mice are the most complete animal model of human immune system reconstruction to date. Therefore, humanized HSC-NOG-EXL mice effectively simulate myeloid cells that are mainly involved in mediating inflammatory reactions, such as allergies and asthma. A humanized mouse model was constructed to study asthmatic airway remodeling and Muc-5ac secretion via human IL-33.[15] Humanized HSC-NOG-EXL mice were exposed to HDM to simulate the pathogenesis of human asthma, and denosumab (full human monoclonal antibody, anti-TNFSF11) was given to further explore the role of TNFSF11.[16]

Establishment of the air-liquid interface (ALI) of primary HBE

This study was approved by the Human Ethics Review Committee (S132) of the First Affiliated Hospital of Shandong First Medical University and conducted after the participants signed informed consent forms. All the participants underwent electronic bronchoscopy, and grades 2–3 bronchial epithelia were collected via lightly brushing with a sterile brush. The obtained HBE cells were placed in a T-25 cm^2 cell culture flask coated with collagen. An appropriate amount of PneumaCult™-Ex medium (STEMCELL Technologies, Vancouver, Canada) was added for culture in the liquid phase, and the changes in cell status were observed. The HBE cells grew outward in clusters on the 4th–6th days and reached 80% confluence on the 10th–12th days. The HBE cells in liquid phase were digested using 0.25% trypsin/ethylenediaminetetraacetic acid (EDTA) and transferred to the air–liquid phase chamber for ALI culture. PneumaCult™-Ex medium was added to the upper and lower Transwell chambers (12 mm and 0.4 μm pore polyester membrane inserts; Corning Inc., Corning, NY, USA). The media in the upper and lower chambers were removed and washed with phosphate-buffered saline (PBS), PneumaCult™-ALI medium (STEMCELL Technologies) was added to the lower chamber, and the HBE cells were cultured in the ALI for more than 20 days. The multilayer cells of the ALI were observed by HE staining under an inverted light lens.[17]

Provisional Provisional

https://doi.org/10.4168/aair.2024.16.e33

HBE cells in exponential growth state were digested with 0.25% trypsin/EDTA, and a cell suspension was prepared with PneumaCult™-Ex complete culture medium. The cell suspension was inoculated in 6-well plates at an appropriate density, and lentiviral transfection was performed when the cell growth and fusion reached approximately 50%–70%. The suspension was divided into lentivirus-*TNFSF11* or *TNFRSF11A* or *TGFβ1* or *TGFβR1* or negative control shRNA groups. Following the lentiviral transfection procedure, a lentiviral vector was mixed with PneumaCult™-EX culture medium and added to a cell flask with HBE cells for transfection. Changes in HBE cells were observed after 12–15 hours of transfection, and the culture medium containing the lentivirus was replaced with PneumaCult™-EX complete culture medium. Puromycin was used to remove the HBE cells that were not transfected with the lentivirus. The cell medium was then changed to PneumaCult after the cells were washed with PBS for the preparation of HBE with low expression. After the cells with the ALI grew to more than 80% of fusion, sterile HDM (50 μg/mL) or rhTNFSF11 protein (50, 100, and 200 ng/mL) was added for 24 hours of stimulation.[18,19] The HBE cells were pretreated with stattic (10 μM/L) for 2 h and then stimulated with rhTNFSF11 (50 ng/mL) for 24 hours.[20] The upper chamber cells were collected for protein analysis. The longitudinal section of the upper chamber cells was collected and fixed with 4% paraformaldehyde, and differentiated HBE sections were prepared by optimum cutting temperature (OCT) embedding for immunofluorescence detection.

Flow cytometry

After the HSC-NOG-EXL mice were anesthetized with isoflurane, their peripheral blood (100 μL) was collected and added to a flow tube. The blood was added with 1 μL of FITC anti-human CD45 (#304005; BioLegend, San Diego, CA, USA) and APC anti-mouse CD45 (#147707; BioLegend). Red blood cells were removed with ammonium–chloride–potassium lysis solution. The mixtures were then centrifuged at 500 ×g for 5 minutes, then the supernatant was discarded. Finally, the cells were suspended with 300 μL of PBS and placed on a FACS LSRII flow cytometer (BD Biosciences, San Jose, CA, USA). Data were analyzed using FlowJo software (Tree Star, Ashland, OR, USA).

Cytokine detection

The mouse peripheral blood was centrifuged at 4°C and 1,000 ×g for 15 minutes, and the supernatant was packaged and stored. The serum TNFSF11 and IgE levels were detected in accordance with the operating procedure of the kit.

The mice were given anesthesia using isoflurane. Their chests were opened, the left main bronchus was ligated and 0.5 mL of sterile PBS was injected into the trachea to collect unilateral bronchoalveolar lavage fluid (BALF). All BALF samples were then centrifuged at 1,000 ×g and 4°C for 20 minutes. The TNFSF11, IL-4, and IL-33 levels in the BALF supernatant were then measured using ELISA kits.

mRNA sequencing

Total RNA of lung tissues was isolated using TRIzol reagent. The samples were enriched for mRNA with polyA structures by using Oligo (dT) magnetic beads. The mRNA was fragmented by divalent cations under elevated temperature in an Illumina proprietary fragmentation buffer. First-strand cDNA was first synthesized using random oligonucleotides and SuperScript II, followed by second-strand cDNA. After the adenylation of the 3′ ends of the DNA fragments, Illumina PE adapter oligonucleotides were ligated to prepare for hybridization. cDNA fragments with a length of 400–500 bp were selected and then purified. DNA fragments with ligated adaptor molecules on both ends were amplified using Illumina PCR primer cocktail in a

Provisional Provisional

Allergy, Asthma & Immunology Research AAIR

15-cycle PCR reaction. Sequencing library construction and RNA-sequencing were carried out by Shanghai Bioprofile Technology Company, Ltd. (Shanghai, China).

Immunohistochemistry

The mouse lung tissues were fixed in 10% neutral formalin, paraffin-embedded, and cut into 5 μm-thick sections. The paraffin sections were antigenically repaired, and endogenous peroxidase was removed and then blocked with 5% bovine serum albumin for 1 hour at 37°C. The slides were incubated with anti-N-cadherin overnight at 4°C and then processed with the corresponding secondary horseradish peroxidase-conjugated antibodies for 30 minutes at room temperature. The sections were stained with 3,3′-diaminobenzidine and hematoxylin dehydrated with a gradient alcohol series, cleared in xylene, and sealed with neutral gum.

Western blot

The cells or lung tissues were fully lysed with radioimmunoprecipitation assay and phenylmethylsulfonyl fluoride lysate. A BCA kit was used to detect protein concentrations in the samples. The proteins were separated through 10% sodium dodecyl sulfate polyacrylamide gel electrophoresis and transferred to polyvinylidene fluoride (PVDF) membranes at low temperatures. The nonspecific binding sites of the PVDF membranes were blocked with 5% bovine milk powder for 1 hour. The PVDF membranes were washed with Tris-buffered saline Tween 20 (TBST) and then incubated with primary antibodies (anti-TNFSF11, anti-TNFRSF11A, anti-N-cadherin, anti-fibronectin, anti-vimentin, anti-collagen I, anti-TGFβ1, anti-p-STAT3, anti-STAT3, anti-p-STAT5, anti-p-STAT6, anti-p-JAK2, IL-4, IL-5, anti-EMBP or anti-GAPDH) at 4°C overnight. On the 2nd day, the PVDF membrane was washed with TBST and incubated with goat anti-rabbit or goat anti-mouse antibody at room temperature for 1 hour. Finally, the PVDF membranes were washed with TBST and exposed with a protein strip. Their proteins were performed with Image J software.

HE staining of HBE in the ALI

The differentiated HBE cells were washed with PBS and fixed with 4% paraformaldehyde for 30 minutes. The cells were cut along the longitudinal section with a sharp blade, embedded in an embedding box with OCT embedding agent, and frozen in a refrigerator at −20°C. The frozen samples were cut into 5 μm-thick pieces with a freezing microtome, and the morphological changes of the cells were observed through HE staining.

Immunofluorescence staining of HBE in the ALI

The 5 μm-thick sections were incubated with goat serum working solution at room temperature for 30 minutes after the cell sections were washed with PBS. A filter paper used to suck the goat serum working fluid, and an antibody (anti-fibronectin, anti-vimentin, anti-collagen I, anti-p-STAT3, anti-TGFβR1) was added to the cell sections, which was then incubated at 4°C overnight. On the 2nd day, the HBE cells were washed with PBS and incubated with a fluorescent secondary antibody. Finally, the sections were stained with DAPI, incubated for 7 minutes, and observed and photographed under a fluorescence microscope.

Lung histology and immunofluorescence

The lungs were embedded in an embedding box with paraffin wax and cut into 5 μm-thick sections. HE and Masson staining were performed as described previously.[4] The lung sections were dewaxed with xylene, dehydrated with gradient concentrations of alcohol, immersed in 0.01 M sodium citrate buffer, and heated to boiling for the heat repair antigen. Goat serum was incubated in the lungs for 40 minutes after liquid cooling. The excess serum working fluid

Provisional Provisional

was removed, and the lung tissues were incubated at 4°C for 24 hours with antibodies (anti-TNFSF11, anti-EPCAM, and anti-p-STAT3, anti-TGFβ1). On the 2nd day, the lung tissues were washed with PBS and incubated with fluorescent secondary antibody and DAPI for 30 minutes. Finally, the lung tissues were observed and photographed under a fluorescence microscope.

Statistical analysis

GraphPad Prism 8.4 and SPSS17.0 were used for statistical tests, and the results were expressed as means ± standard deviation of at least 3 biological duplications. *P* value < 0.05 indicated statistically significant difference. The *t*-test (normally distributed parameters) or Mann–Whitney *U* test (non-normally distributed parameters) was used to evaluate statistical significance for the two groups. The normally distributed parameters of one-way analysis of variance (ANOVA) and Welch ANOVA and non-normally distributed parameters of Kruskal–Wallis test were used in evaluating statistical significance for multiple comparisons. Correlations were determined by Spearman analysis.

RESULTS

Elevated TNFSF11 expression in asthmatic serum as determined by Olink inflammation-related biomarker analysis

Olink inflammatory biomarker was used to evaluate the expression levels of inflammatory-associated proteins (n = 92) in the asthmatic and normal groups. DEPs were identified between the asthmatic and normal groups; among which, 11 proteins in the asthma group were up-regulated, and TNFSF11expression significantly increased (**Fig. 1A**). Interprotein correlation analysis was performed to explore interactions between different proteins. TNFSF11, IL-6, and TNF were highly rated in the PPI network (**Fig. 1B**). IL-6 and TNF play an important role in asthma progression.[4,21] GO and KEGG enrichment analyses were performed on the background of DEPs. The results showed that the functions of TNFSF11 were mainly concentrated in extracellular space and region, immune response, and signaling molecule interaction (**Fig. 1C and D**). Therefore, TNFSF11 plays an important role in asthma.

Elevated TNFSF11 expression in bronchial epithelium and serum from asthmatic subjects

Endoscopic specimens were collected from healthy individuals and patients with asthma. The asthmatic subjects had collagen deposition around the airway compared with the normal group (**Fig. 2A and C**). Immunohistochemical results indicated that TNFSF11 protein levels significantly increased in the bronchial epithelia of the patients with asthma relative to those in healthy individuals (**Fig. 2B and D**). Subsequently, this study also analyzed TNFSF11 in serum from asthmatic and normal subjects using ELISA. This study verified that serum TNFSF11 level in asthmatic subjects was significantly higher after the number of samples was increased (**Fig. 2E**). The correlation of eosinophil cells (Eos) and lung function with TNFSF11 was then analyzed. The TNFSF11 level in serum was positively correlated with Eos (**Fig. 2F**) and negatively correlated with forced vital capacity (FVC), forced expiratory volume in 1 second (FEV1) % and FEV1/FVC (**Fig. 2G-I**). In summary, TNFSF11 is associated with asthma.

Elevated TNFSF11 expression in the BALF, sera, and bronchial epithelia of mice with HDM-induced asthma

The animal models are shown in **Fig. 3A**.[22] Serum IgE, Eos number and percentage, and BALF IL-33 level were significantly aggravated in the mice with HDM-induced asthma (**Fig. 3B-E**).

Provisional Provisional

Allergy, Asthma & Immunology Research AAIR

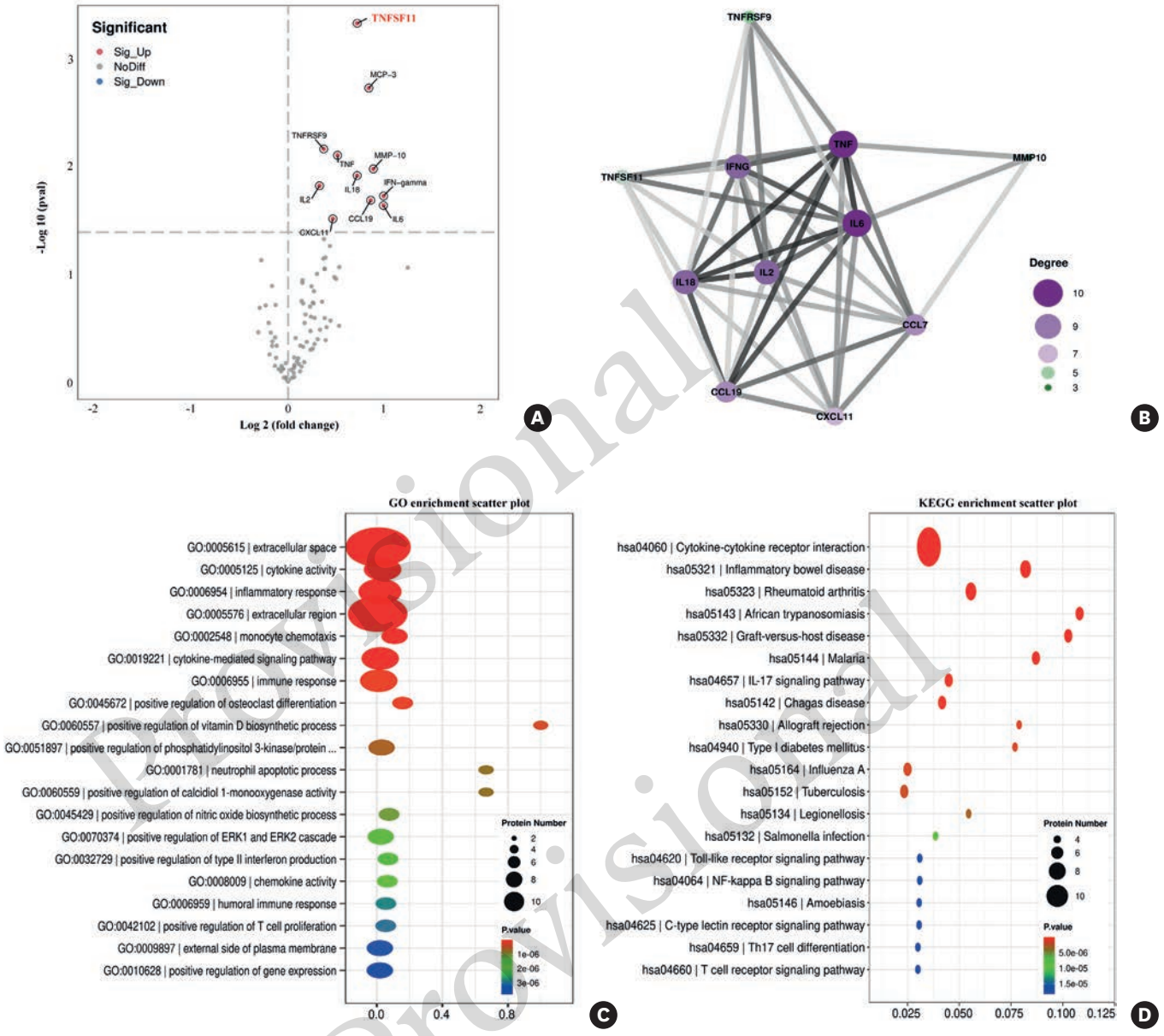

Fig. 1. DEPs among inflammation-related biomarkers between the asthmatic (n = 11) and normal (n = 10) groups. (A) Volcano plot of DEPs, including TNFSF11. (B) PPI network analysis of TNFSF11. (C) GO enrichment analysis with scatter plot. (D) KEGG enrichment analysis with scatter plot.
DEP, differentially expressed protein; TNFSF11, TNF ligand superfamily member 11; PPI, protein-protein interaction; GO, Gene Ontology; KEGG, Kyoto Encyclopedia of Genes and Genomes.

Provisional

Inflammatory cell infiltration and collagen deposition were elevated (**Fig. 3F and G**), and *Tnfsf11* mRNA (**Fig. 3H**) and protein levels were significantly elevated (**Fig. 3I and J**). We further examined TNFSF11 expression in the sera and found higher levels in the asthmatic model than in normal mice (**Fig. 3K**). Immunofluorescence double staining confirmed that TNFSF11expression was elevated in the airway epithelia of the asthmatic mice compared with that in the normal mice (**Fig. 3L and M**). Finally, BALF TNFSF11 level in the asthmatic model was higher than that in the normal mice (**Fig. 3N**). In conclusion, TNFSF11 level is associated with HDM-induced asthma in mice.

https://doi.org/10.4168/aair.2024.16.e33

Allergy, Asthma & Immunology Research AAIR

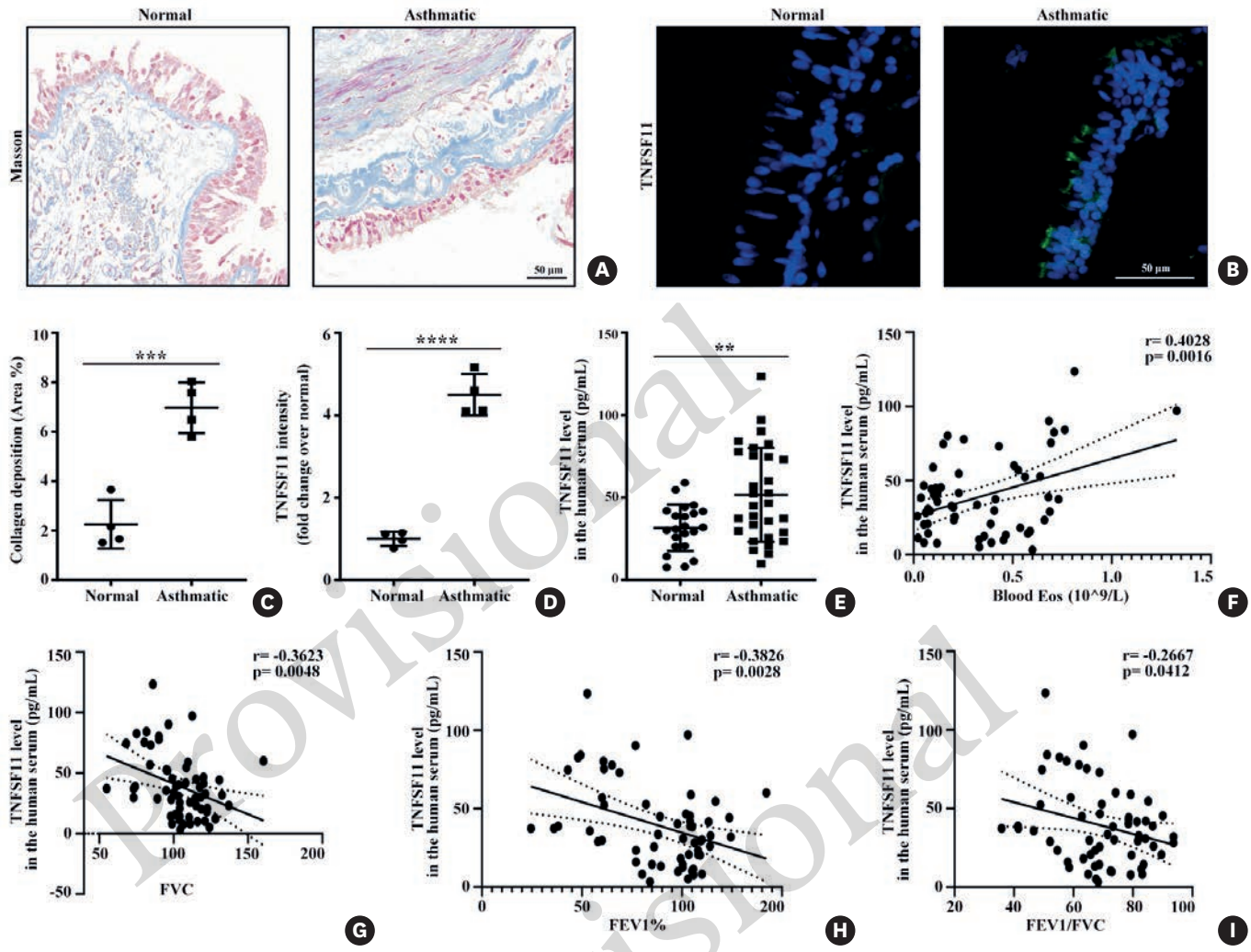

Fig. 2. Elevated TNFSF11 expression in human specimens of airway and serum. (A) Collagen deposition measured by Masson staining. (B) TNFSF11 expression measured by immunofluorescent staining. (C) Quantification of collagen volume fraction. (D) Quantification of TNFSF11 intensity. (E) serum TNFSF11 in the asthmatic (n = 37) and normal (n = 22) groups measured by ELISA. (F) Correlation analysis between serum TNFSF11 and Eos. (G) Correlation analysis between serum TNFSF11 and FVC. (H) Correlation analysis between serum TNFSF11 and FEV1%. (I) Correlation analysis between serum TNFSF11 and FEV1/FVC. Magnification 200×, scale bar: 50 μm. Data are expressed as means ± standard deviation of 3 independent experiments.
TNFSF11, TNF ligand superfamily member 11; ELISA, enzyme-linked immunosorbent assay; Eos, eosinophil cells; FVC, forced vital capacity; FEV1, forced expiratory volume in 1 second.
*P < 0.05, **P < 0.01, ***P < 0.001, ****P < 0.0001.

Provisional Provisional

Elevated TNFSF11 protein level promotes airway remodeling

Next, we intranasally administered rmTNFSF11 active protein to the mice (**Fig. 4A**). HE and PAS staining results indicated that inflammatory cells aggregated around the airway and epithelial mucus secretion was upregulated after rmTNFSF11 protein stimulation (**Fig. 4B, C, F, and G**). Masson staining results indicated that a large amount of collagen was deposited around the airway after the intranasal administration of rmTNFSF11 protein (**Fig. 4D and H**). N-cadherin histochemistry and western blot results further confirmed that rmTNFSF11 protein induced mouse airway remodeling (**Fig. 4E, I, J-M**). In conclusion, TNFSF11 protein promotes mucus secretion, accelerating airway remodeling.

https://doi.org/10.4168/aair.2024.16.e33

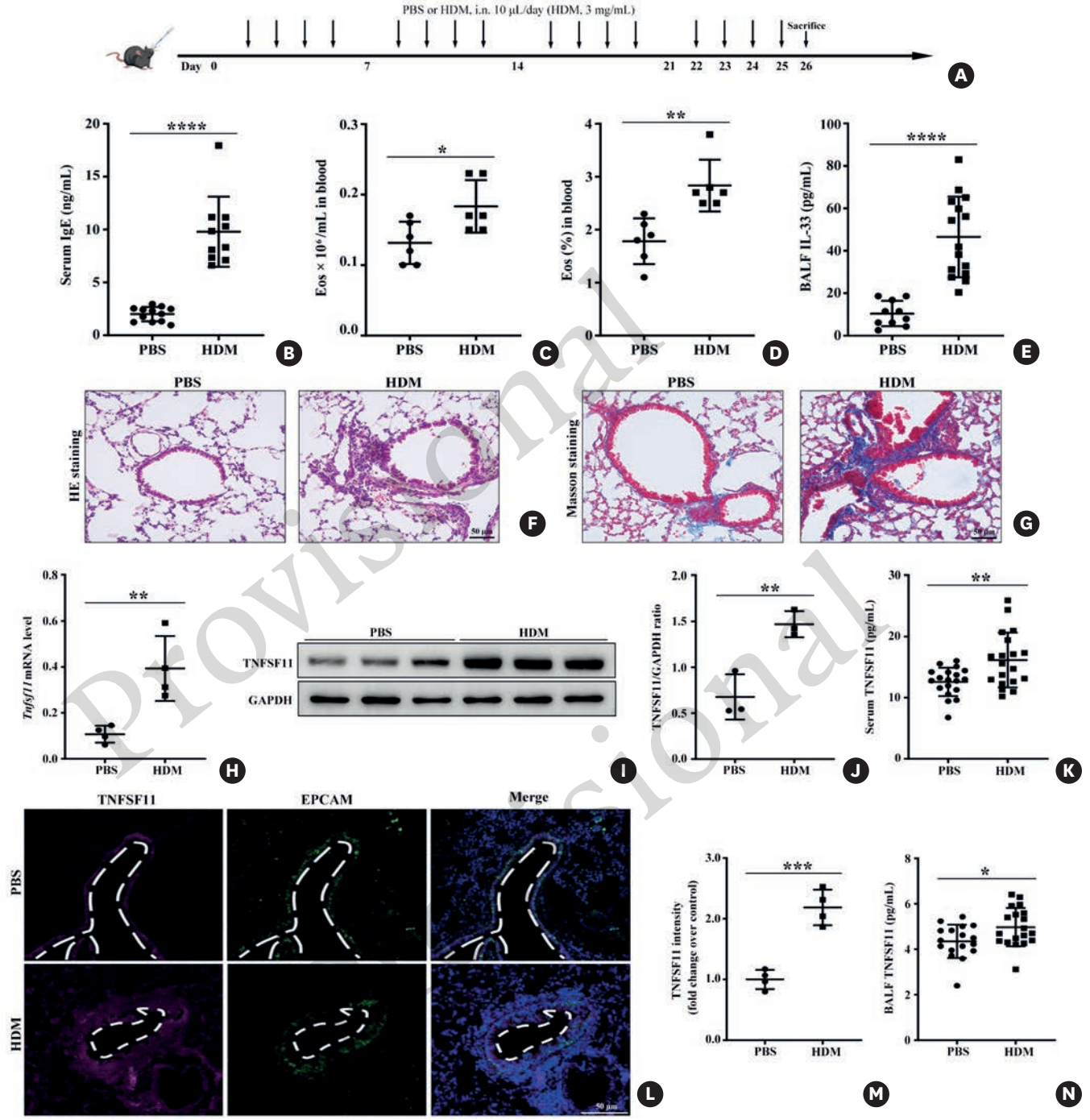

Fig. 3. Increased TNFSF11 expression in mice with HDM-induced asthma. (A) Animal schedule of HDM-induced asthma model (n = 6). (B) Serum IgE detected by ELISA. (C, D) Number of Eos measured by hematologic cell analysis. (E) IL-33 levels in BALF detected by ELISA. (F) HE staining, (G) Masson-stained lung tissues. Magnification 200×, scale bar: 50 μm. (H) *Tnfsf11*mRNA level in mice with HDM-induced asthma. (I) TNFSF11 level in mice with HDM-induced asthma evaluated by Western blot. (J) TNFSF11/GAPDH ratio. (K) Mouse serum TNFSF11 detected by ELISA. (L) Immunofluorescence staining of TNFSF11 and EPCAM from mouse lungs. (M) TNFSF11 intensity analysis. (N) BALF TNFSF11 detected by ELISA. Data are expressed as means ± standard deviation of 3 independent experiments.
TNFSF11, TNF ligand superfamily member 11; HDM, house dust mite; Ig, immunoglobulin; ELISA, enzyme-linked immunosorbent assay; Eos, eosinophil cells; IL, interleukin; BALF, bronchoalveolar lavage fluid; HE, hematoxylin–eosin; GAPDH, glyceraldehyde 3-phosphate dehydrogenase; PBS, phosphate-buffered saline.
$^{*}P < 0.05$, $^{**}P < 0.01$, $^{***}P < 0.001$, $^{****}P < 0.0001$.

Provisional

https://doi.org/10.4168/aair.2024.16.e33

Allergy, Asthma & Immunology Research AAIR

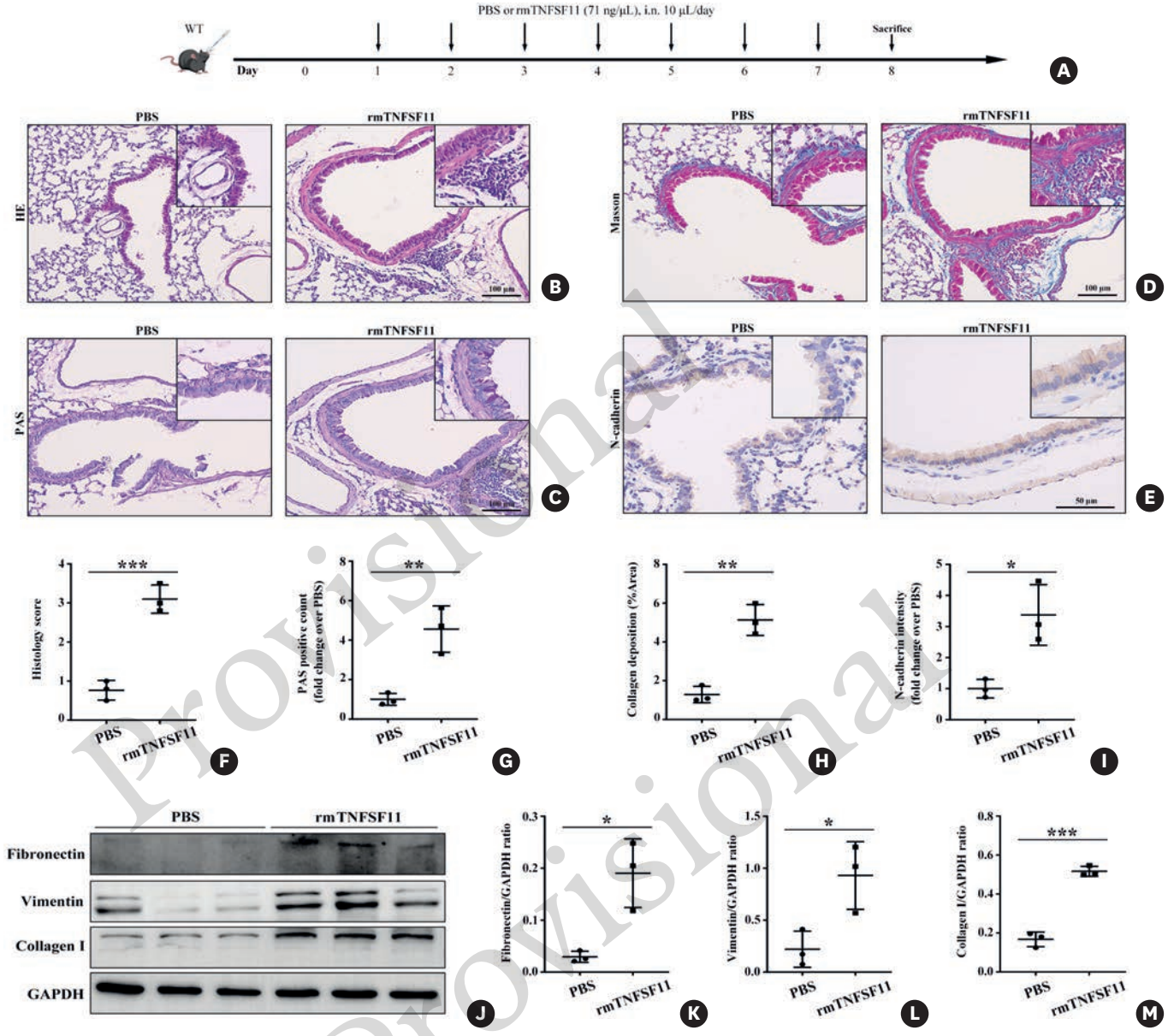

Provisional

Fig. 4. TNFSF11 promoted airway inflammatory responses and remodeling. (A) Animal experimental schedule (n = 6). (B) HE, (C) PAS, (D) Masson, and (E) N-cadherin staining. Magnification 100×, scale bar: 100 μm. Magnification 200×, scale bar: 50 μm. (F-I) Intensity analysis of (B-E). (J) Changes of fibronectin, vimentin, and collagen I in rmTNFSF11-induced mice evaluated by Western blot. (K-M) Relative protein level of (J). Data are expressed as the means ± standard deviation of 3 independent experiments.
TNFSF11, TNF ligand superfamily member 11; HE, hematoxylin–eosin; PAS, periodic acid–Schiff; WT, wild type; PBS, phosphate-buffered saline; GAPDH, glyceraldehyde 3-phosphate dehydrogenase.
*P < 0.05, **P < 0.01, ***P < 0.001, ****P < 0.0001.

TNFSF11/TNFRSF11A axis deficiency alleviates HDM-induced airway remodeling

The effect of TNFSF11/TNFRSF11A axis in the *Tnfsf11* and *Tnfrsf11a* mice with HDM-induced asthma was further verified (**Figs. 5A** and **6A**). Western blot results confirmed that TNFSF11/TNFRSF11A axis deficiency reduced the expression levels of N-cadherin, vimentin, and collagen I in mice with HDM-induced asthma (**Figs. 5B-5F** and **6B-6F**). In particular, BALF IL-4 and serum IgE were significantly lower in the *Tnfsf11* and *Tnfrsf11a* mice with HDM-induced asthma than in the wild type (WT) mice with HDM-induced asthma (**Figs. 5G**, **5H**,

https://doi.org/10.4168/aair.2024.16.e33

Allergy, Asthma & Immunology Research AAIR

6G, and **6H**). Finally, HE and Masson staining results showed that pathological injury and collagen deposition decreased in the *Tnfsf11* and *Tnfrsf11a* mice with HDM-induced asthma than in the WT mice with HDM-induced asthma (**Figs. 5I**, **5J**, **6I**, and **6J**).

TNFSF11/TNFRSF11A axis activates STAT3 signaling in mice with HDM-induced asthma

Messenger RNA transcription was analyzed in the WT and HDM-induced *Tnfsf11*$^{+/-}$ mice with HDM-induced asthma. Volcanic maps showed the expression levels of some differential genes (**Fig. 7A**). Functional enrichment of differential genes showed that TNFSF11 played an important role in the extracellular region, and the function that might be related to the JAK-STAT signaling pathways (**Fig. 7B**). Western blot results showed that STAT3 phosphorylation levels significantly decreased in the *Tnfsf11* and *Tnfrsf11a* mice with HDM-induced asthma than in the WT mice with HDM-induced asthma (**Fig. 7C-F**). However, the phosphorylation levels of STAT5, STAT6, and JAK showed no change in the *Tnfsf11* mice with HDM-induced asthma than in the WT mice with HDM-induced asthma (**Fig. 7C**). Finally, immunofluorescence co-localization results revealed a significant reduction in STAT3 phosphorylation in the airway epithelium of the *Tnfsf11* mice with HDM-induced asthma than in the WT mice with HDM-induced asthma (**Fig. 7G and H**). In conclusion, TNFSF11/TNFRSF11A deficiency ameliorates HDM-induced asthma via the p-STAT3 signaling pathway.

TNFSF11/TNFRSF11A axis activates STAT3 signaling in HDM-stimulated HBE

TNFSF11 binding with TNFRSF11A activates downstream signaling. Therefore, TNFSF11/TNFRSF11A axis in HBE were interrupted by *TNFSF11* or *TNFRSF11A* shRNA (**Fig. 8A**). The decrease in HDM-induced STAT3 phosphorylation was larger in HDM+*TNFSF11* shRNA group than in the HDM group (**Fig. 8B and C**). *TNFSF11* shRNA decreased the HDM-induced expression of vimentin and collagen I (**Fig. 8B, D, and E**). In addition, the STAT3 phosphorylation level in the HDM+*TNFRSF11A* shRNA group was lower than that in the HDM group (**Fig. 8F and G**). *TNFRSF11A* shRNA also decreased the HDM-induced expression of fibronectin and collagen I (**Fig. 8F, H, and I**).

TNFSF11/TNFRSF11A axis aggravated airway remodeling by TGFβ1/STAT3 action

We further added different concentrations of TNFSF11 (50, 100, and 200 ng/mL) to stimulate HBE cells. Western blot results showed that TGFβ1, fibronectin, vimentin, and collagen I levels significantly increased under TNFSF11 (50 ng/mL) stimulation (**Fig. 9A-E**). HBE cells were pretreated with stattic[20] and then stimulated with rhTNFSF11. Stattic decreased the levels of collagen I and vimentin by inhibiting STAT3 phosphorylation (**Fig. 9F-I**).

Next, we constructed *TGFβ1* or *TGFβR1* shRNA to further verify the role of TGFβ1/TGFβR1 in STAT3 phosphorylation and remodeling induced by TNFSF11. The TGFβ1 expression decreased in the TNFSF11-stimulated HBE cells with *TGFβ1* shRNA compared with that in the TNFSF11-stimulated HBE cells (**Fig. 9J and K**). The levels of STAT3 phosphorylation, vimentin, and collagen I significantly decreased in the TNFSF11-stimulated HBE cells with *TGFβ1* shRNA (**Fig. 9J, L-N**). Finally, HBE cells were stained to locate TGFβR1 expression, STAT3 phosphorylation, remodeling proteins (**Fig. 9O**). TGFβR1 expression and STAT3 phosphorylation decreased in the TNFSF11-stimulated HBE cells with *TGFβR1* shRNA compared with that in the TNFSF11-stimulated HBE cells (**Fig. 9P and Q**). The levels of fibronectin, vimentin, and collagen I significantly decreased in the TNFSF11-stimulated HBE cells with *TGFβR1* shRNA compared with those in the HDM-stimulated HBE cells (**Fig. 9R-T**).

Provisional Provisional

https://doi.org/10.4168/aair.2024.16.e33

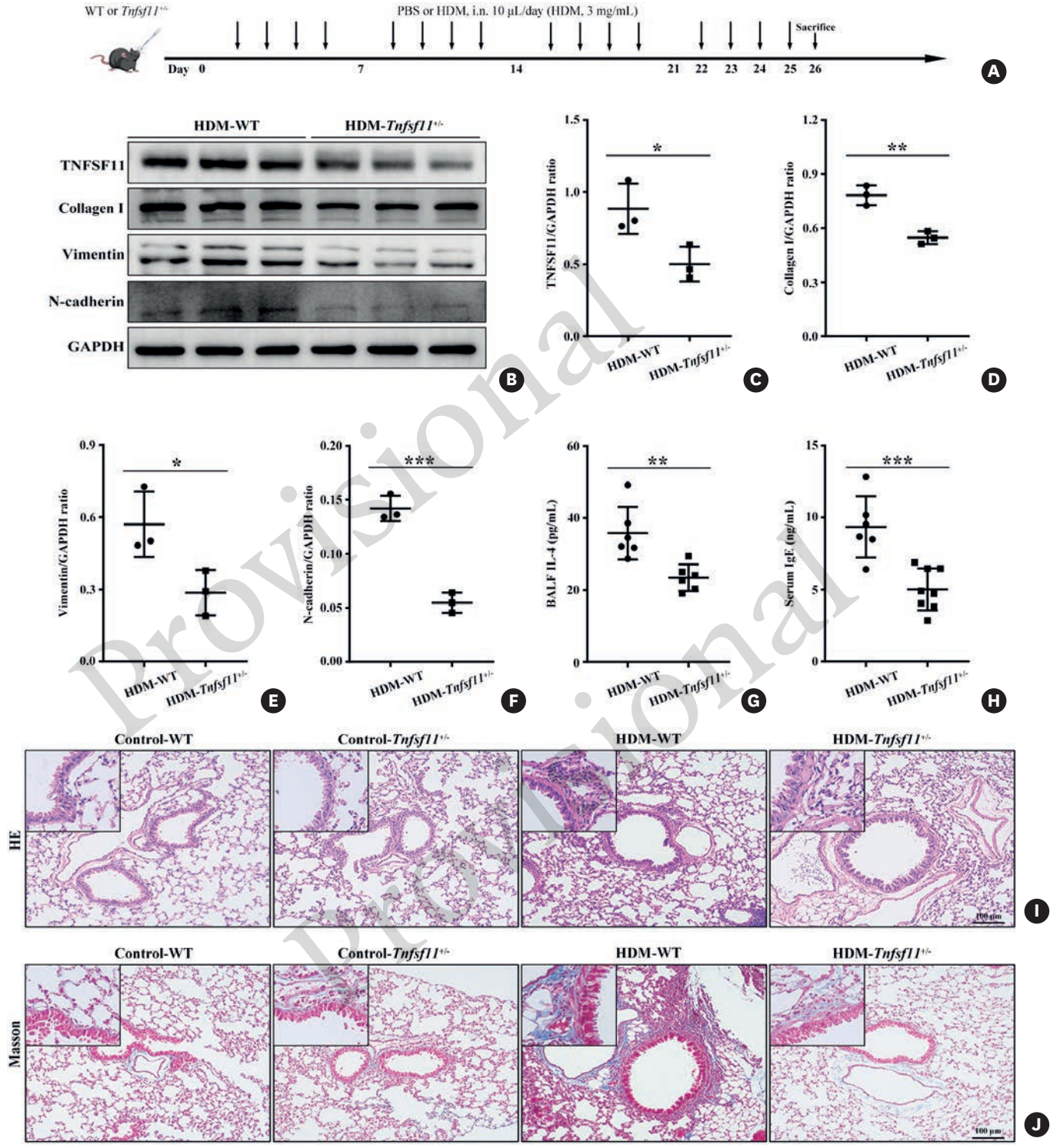

Fig. 5. *Tnfsf11*$^{+/-}$ alleviated HDM-induced asthma. (A) Strategy for HDM-induced asthma in *Tnfsf11*$^{+/-}$ mice (n = 6). (B) Effects of the *Tnfsf11*$^{+/-}$ on HDM-induced collagen I, vimentin, and N-cadherin verified by Western blot. (C-F) Relative protein level analysis. (G) BALF IL-4 and (H) Serum IgE detected by ELISA. (I) Effects of the *Tnfsf11*$^{+/-}$ on HDM-induced inflammation detected by HE staining. (J) Effects of the *Tnfsf11*$^{+/-}$ on HDM-induced airway remodeling detected by Masson staining. Magnification 100×, scale bar: 100 μm. Data are expressed as the means ± standard deviation of 3 independent experiments.
TNFSF11, TNF ligand superfamily member 11; HDM, house dust mite; BALF, bronchoalveolar lavage fluid; IL, interleukin; Ig, immunoglobulin; ELISA, enzyme-linked immunosorbent assay; HE, hematoxylin–eosin; WT, wild type; PBS, phosphate-buffered saline; GAPDH, glyceraldehyde 3-phosphate dehydrogenase.
*P < 0.05, **P < 0.01, ***P < 0.001, ****P < 0.0001.

Provisional

https://doi.org/10.4168/aair.2024.16.e33

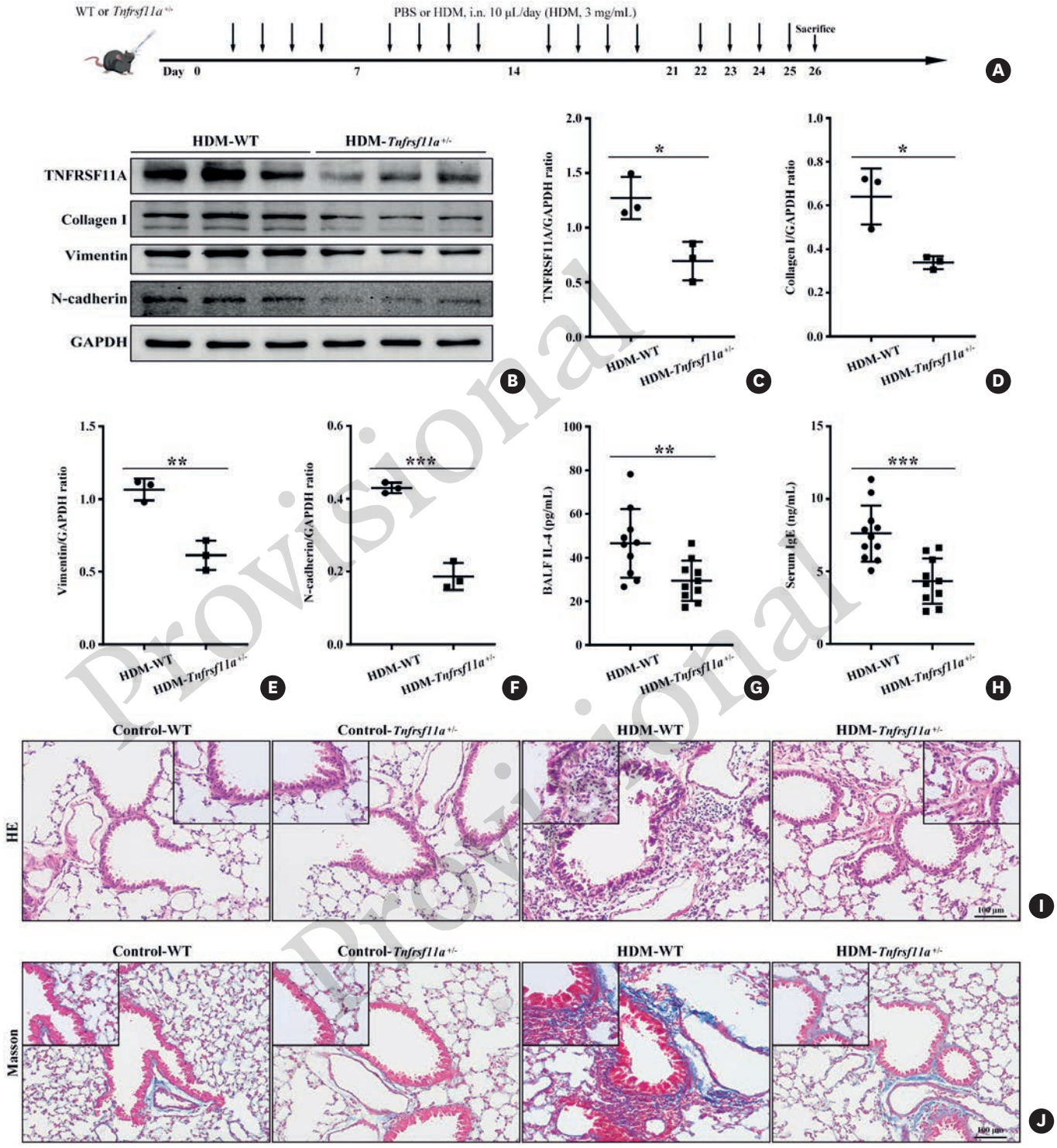

Fig. 6. *Tnfrsf11a*$^{+/-}$ alleviated HDM-induced asthma. (A) Strategy for HDM-induced asthma in *Tnfrsf11a*$^{+/-}$ mice (n = 6). (B) Effects of the *Tnfrsf11a*$^{+/-}$ on HDM-induced collagen I, vimentin, and N-cadherin verified by Western blot. (C-F) Relative protein level of (B). (G) BALF IL-4 and (H) Serum IgE detected by ELISA. (I) Effects of the *Tnfrsf11a*$^{+/-}$ on HDM-induced inflammation detected by HE staining. (J) Effects of the *Tnfrsf11a*$^{+/-}$ on HDM-induced airway remodeling detected by Masson staining. Magnification 100×, scale bar: 100 μm. Data are expressed as the means ± standard deviation of 3 independent experiments.
TNFRSF11A, TNF receptor superfamily 11A; HDM, house dust mite; BALF, bronchoalveolar lavage fluid; IL, interleukin; Ig, immunoglobulin; ELISA, enzyme-linked immunosorbent assay; HE, hematoxylin–eosin.
$^{*}P < 0.05$, $^{**}P < 0.01$, $^{***}P < 0.001$, $^{****}P < 0.0001$.

Provisional

https://doi.org/10.4168/aair.2024.16.e33

Allergy, Asthma & Immunology Research AAIR

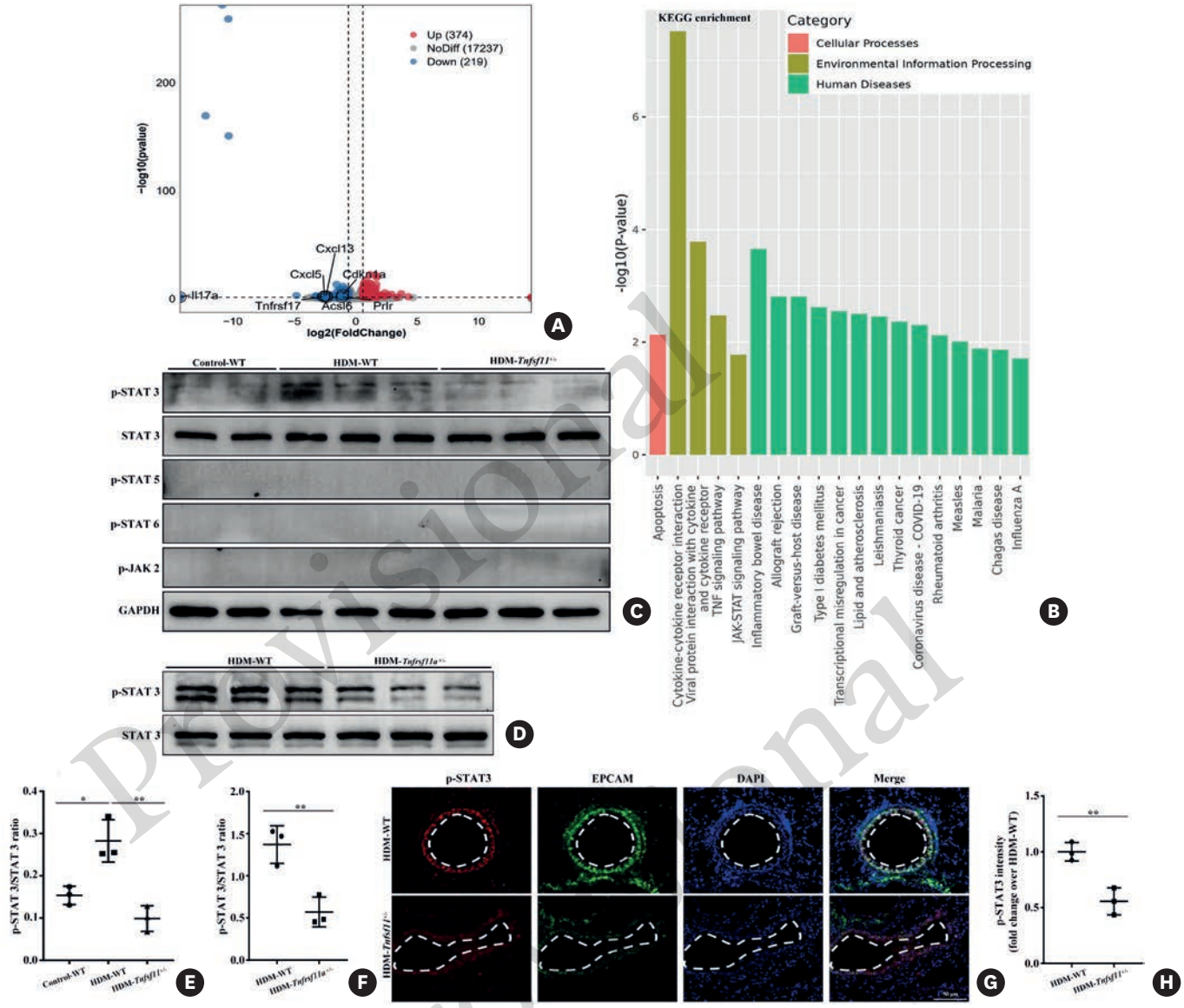

Fig. 7. STAT3 signaling involved in HDM-induced asthma in *Tnfsf11*$^{+/-}$ or *Tnfrsf11a*$^{+/-}$ mice (n = 6). (A) Volcano plots for screening differential expression proteins with thresholds of $P < 0.05$ and fold change > 2. (B) KEGG enrichment after HDM-induced *Tnfsf11*$^{+/-}$ vs. HDM-induced WT. (C, D) Enriched signaling pathway of JAK-STAT validated by Western blot. (E) p-STAT3/STAT3 ratio in mice with HDM-induced *Tnfsf11*$^{+/-}$ vs. HDM-induced WT. (F) p-STAT3/STAT3 ratio in mice with HDM-induced *Tnfrsf11a*$^{+/-}$ vs. HDM-induced WT. (G) The p-STAT3 and EPCAM around the airway epithelium in *Tnfsf11*$^{+/-}$ mice with HDM-induced asthma measured by double-labeling immunofluorescence. Magnification 200×, scale bar: 50 μm. (H) p-STAT3 intensity analysis. Data are expressed as the means ± standard deviation of 3 independent experiments.
STAT3, signal transducer and activator of transcription 3; HDM, house dust mite; TNFSF11, TNF ligand superfamily member 11; TNFRSF11A, TNF receptor superfamily 11A; KEGG, Kyoto Encyclopedia of Genes and Genomes; WT, wild type.
*$P < 0.05$, **$P < 0.01$, ***$P < 0.001$, ****$P < 0.0001$.

Denosumab improves HDM-induced asthma in humanized HSC-NOG-EXL mice by inhibiting TGFβ1/STAT3 action

Flow cytometry results showed that human CD45 was more than 50% after 7 weeks of human CD34+huHSC transplantation (**Supplementary Fig. S2**). The effect of denosumab was further verified in the humanized HSC-NOG-EXL mice with HDM-induced asthma (**Fig. 10A**). Western blot analysis showed that denosumab significantly inhibited or neutralized HDM-induced TNFSF11 expression, but had no effect on HDM-induced TNFRSF11A expression in the HSC-NOG-EXL mice (**Fig. 10B-D**). IL-4 cytokine level significantly decreased in the HDM

Provisional Proof

https://doi.org/10.4168/aair.2024.16.e33

Allergy, Asthma & Immunology Research AAIR

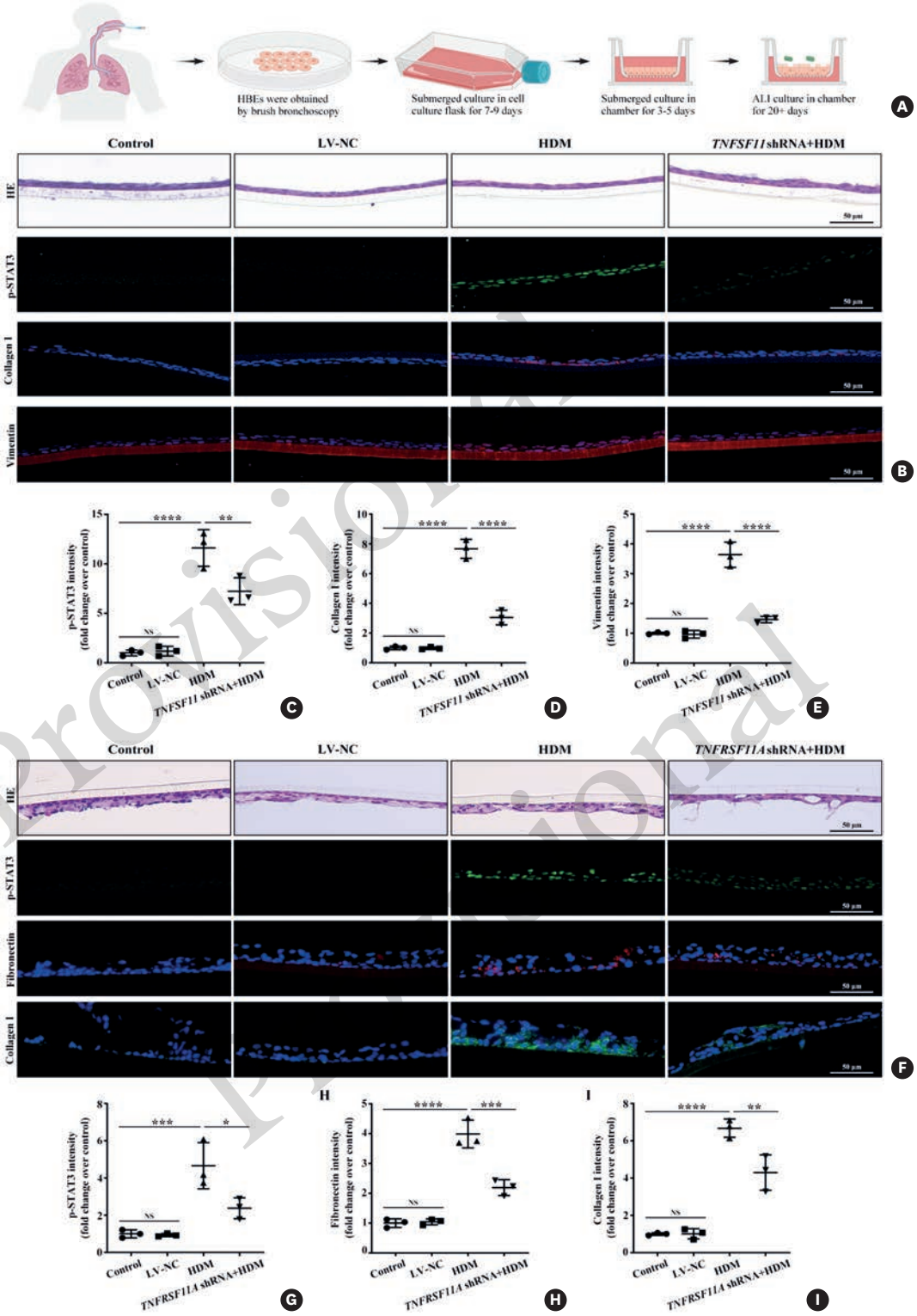

Fig. 8. Intervention on TNFSF11/TNFRSF11A axis alleviated HDM-induced remodeling proteins with HBE cells by STAT3 phosphorylation. (A) Strategy for cell models. (B-E) Effects of *TNFSF11* shRNA on HDM-stimulated HE, p-STAT3, collagen I, and vimentin. (F-I) Further analysis on the effects of *TNFRSF11A* shRNA on HDM-stimulated HE, p-STAT3, fibronectin, and collagen I. Magnification 200×, scale bar: 50 μm. Data are expressed as the means ± standard deviation of 3 independent experiments.
TNFSF11, TNF ligand superfamily member 11; TNFRSF11A, TNF receptor superfamily 11A; HDM, house dust mite; HBE, human bronchial epithelial; STAT3, signal transducer and activator of transcription 3; shRNA, short hairpin RNA; HE, hematoxylin–eosin; LV-NC, negative control lentivirus; NS, not significant.
$^{*}P < 0.05$, $^{**}P < 0.01$, $^{***}P < 0.001$, $^{****}P < 0.0001$.

Provisional

https://doi.org/10.4168/aair.2024.16.e33

Allergy, Asthma & Immunology Research AAIR

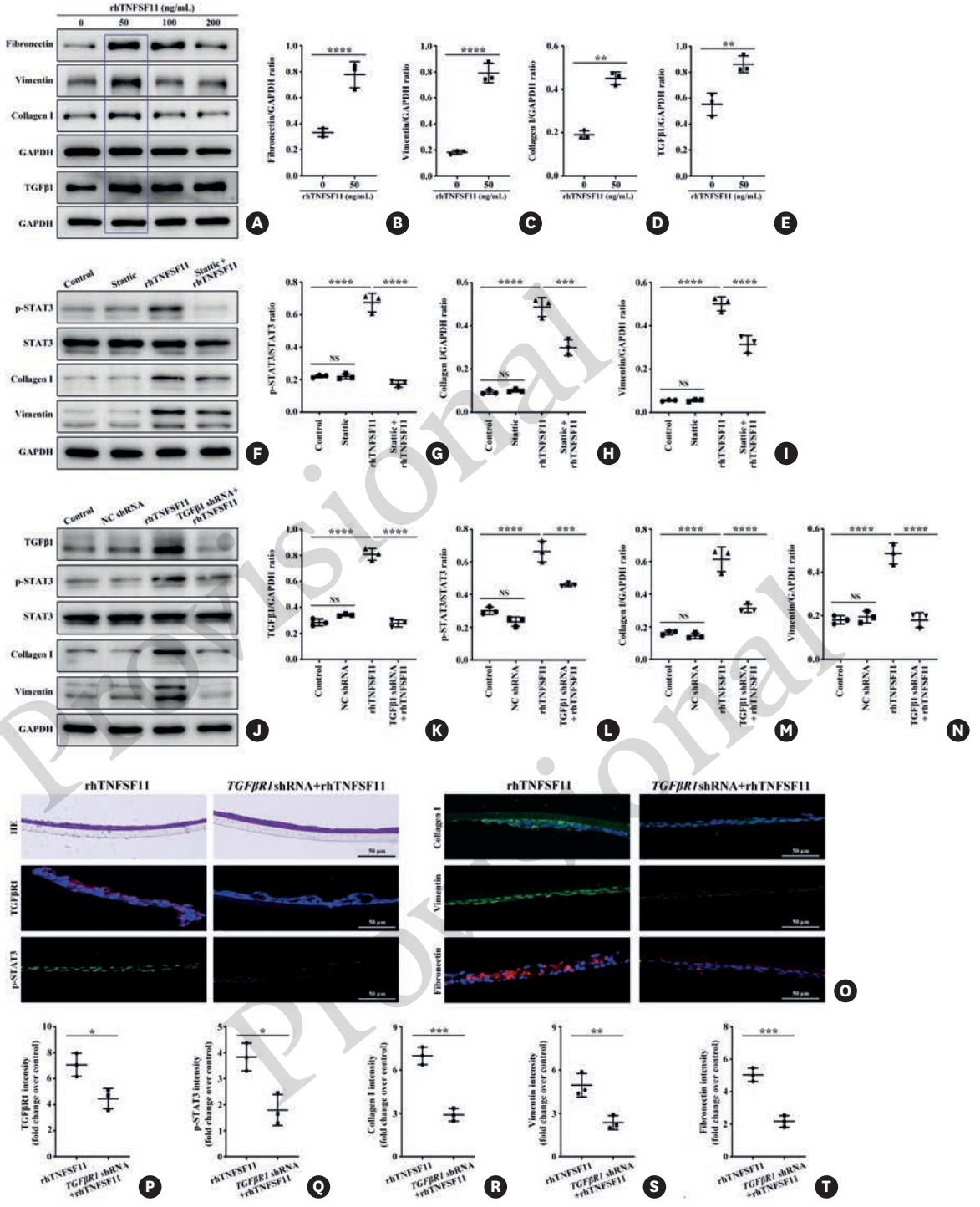

Fig. 9. TNFSF11 promoted airway remodeling by TGFβ1/STAT3 signaling. (A-E) Remodeling proteins and TGFβ1 in rhTNFSF11-stimulated HBE cells evaluated by Western blot. rhTNFSF11 (50 ng/mL) selected to stimulate HBE cells. (F-I) Intervention with STAT3 phosphorylation used by stattic to further explore the role of STAT3 phosphorylation in remodeling proteins. (J-N) Intervention with TGFβ1 used by lentivirus to further explore the role of TGFβ1 signaling in STAT3 phosphorylation and remodeling proteins. (O) HBE staining of HE, TGFβR1, p-STAT3, collagen I, vimentin, and fibronectin in the rhTNFSF11-stimulated HBE cells with *TGFβR1* shRNA. (P-T) Fluorescence intensity analysis. Magnification 200×, scale bar: 50 μm.
TNFSF11, TNF ligand superfamily member 11; TGFβ1, transforming growth factor β1; STAT3, signal transducer and activator of transcription 3; HBE, human bronchial epithelial; HE, hematoxylin–eosin; GAPDH, glyceraldehyde 3-phosphate dehydrogenase; NS, not significant.
$^{*}P < 0.05$, $^{**}P < 0.01$, $^{***}P < 0.001$, $^{****}P < 0.0001$.

Provisional Proof

https://doi.org/10.4168/aair.2024.16.e33

+ denosumab group compared with those in the HDM group (**Fig. 10B and E**). IL-5 cytokine level showed no change between the HDM + denosumab and HDM groups (**Fig. 10B and F**). The EMBP expression decreased in the HDM + denosumab group compared with that in the HDM group (**Fig. 10B and G**).

HE and PAS results showed that denosumab significantly reduced the accumulation of HDM-induced inflammatory cells into the airway and the airway secretion of mucus (**Fig. 10H, I, M, and N**). Masson staining further demonstrated that denosumab significantly inhibited HDM-induced airway collagen deposition (**Fig. 10J and O**), TGFβ1 level, and STAT3 phosphorylation in the HSC-NOG-EXL mice (**Fig. 10K, L, P, and Q**). Overall, denosumab decreases TGFβ1 level and STAT3 phosphorylation in the HSC-NOG-EXL mice with HDM-induced asthma.

DISCUSSION

This study first revealed that TNFSF11 levels were significantly elevated in asthmatic human specimens by analyzing serum and airway epithelium. The TNFSF11/TNFRSF11A axis activates TGFβ1/STAT3 signaling to exacerbate asthmatic airway remodeling (**Fig. 11**). The HDM-induced HSC-NOG-EXL asthmatic model provides a solid foundation and novel strategy for denosumab treatment of asthma.

TNFSF11 has an originally important role in resorption and remodeling in the bone metabolic disease.[23] This role has gradually extended to lung diseases. TNFSF11/TNFRSF11A is an important signaling pathway in dendritic cells.[12,24,25] After dendritic cells present antigens to naive T cells in mediastinal lymph nodes, specific $CD4^+$T cells activate, expand, and differentiate specifically into Th2 cells, which then migrate to the lungs and coordinate the pulmonary immune response. Dendritic cells induce antigen-specific Th2 cell activation during asthma development. Hence, blocking TNFSF11/TNFRSF11A interaction might reduce the effective function of dendritic cells, thereby reducing the presentation of allergens to naive T cells. However, research on asthma is not comprehensive, and the specific mechanism of TNFSF11 in asthma airway remodeling remains unknown. The present study revealed that the TNFSF11/TNFRSF11A axis activates TGFβ1/STAT3 signaling and thereby exacerbates asthma development in airway remodeling. In addition, glucocorticoids play an important role in asthma treatment, but one of their side effects is abnormal bone metabolism.[26-28] Denosumab can be used to the treat glucocorticoid-induced osteoporosis.[29] TNFSF11/TNFRSF11A is involved in the occurrence of asthma and plays an important role in the treatment of asthma with glucocorticoids. The results provided a solid theoretical basis for the use of denosumab as asthma treatment and the alleviation of the side effects of glucocorticoid treatment for asthma.

HDM is a common causative factor of asthma; its components are relatively complex and can destroy the tight junctions between cells, leading to the production and release of cytokines and chemokines, and ultimately airway remodeling and mucus hypersecretion.[30,31] Airway epithelial dysfunction is the premise of epithelial-mesenchymal crosstalk. Airway epithelial function depends on cell integrity and the coordinated expression and interaction between cell-cell junction complexes, especially tight junction proteins. Patients with asthma allergy exhibit epithelial dysfunction associated with tight junctions.[32,33] Occludin is a key component of tight junction proteins, and protein kinase C (PKC), Src, tyrosine kinase 2, phospholipase C

Provisional

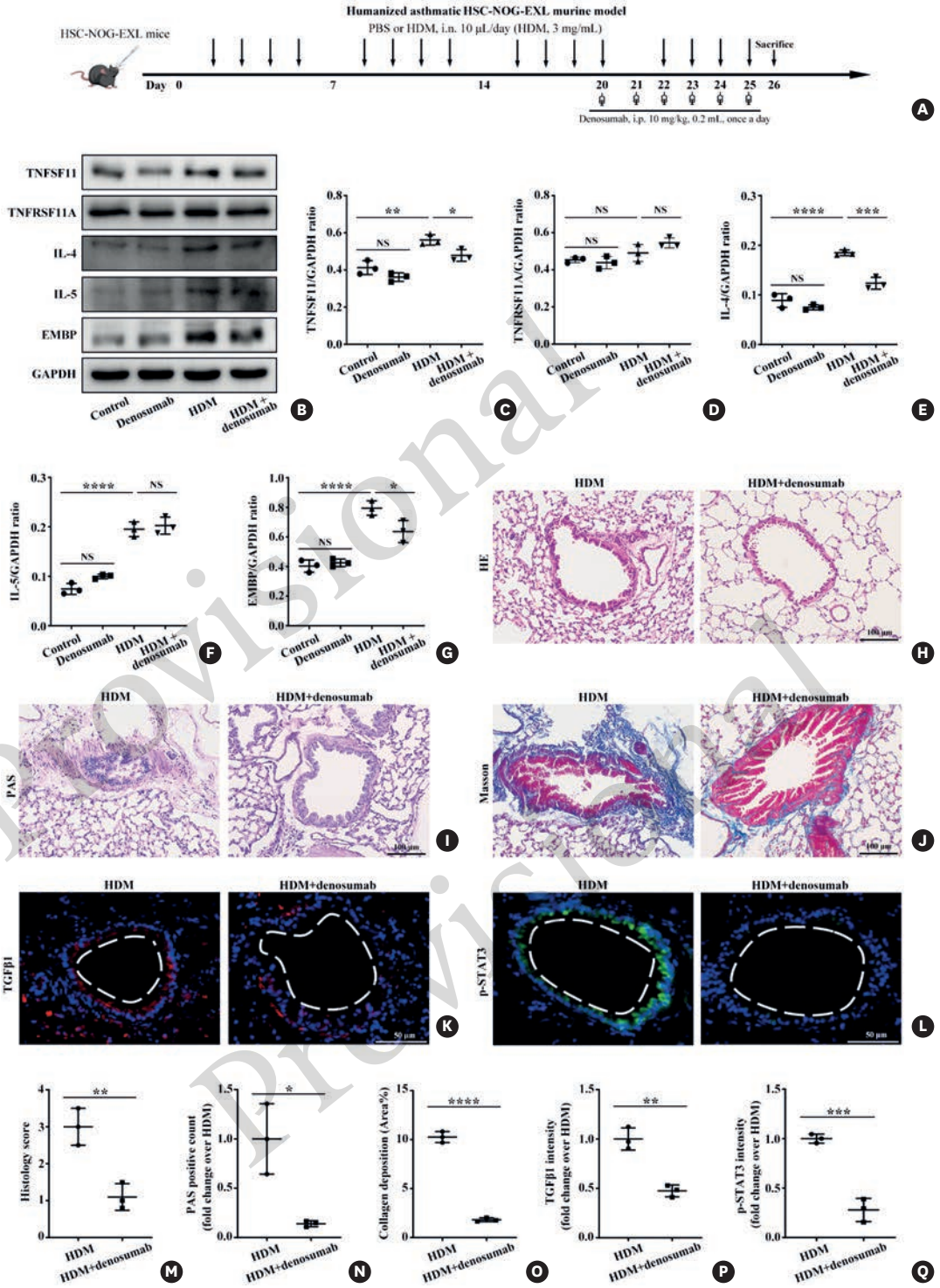

Fig. 10. Effects of denosumab (anti-human TNFSF11) on HDM-induced humanized HSC-NOG-EXL murine. (A) Strategy for HDM-induced asthma in HSC-NOG-EXL murine (n = 6). (B) Western blot analysis of TNFSF11, TNFRSF11A, IL-4, IL-5, and EMBP. (C) TNFSF11/GAPDH ratio. (D) TNFRSF11A/GAPDH ratio. (E) IL-4/GAPDH ratio. (F) IL-5/GAPDH ratio. (G) EMBP/GAPDH ratio. (H) HE, (I) PAS, (J) Masson staining to examine the effects of denosumab on HSC-NOG-EXL mice with HDM-induced asthma. (K) Mouse lungs stained with TGFβ1 by immunofluorescence. (L) Mouse lungs stained with p-STAT3 by immunofluorescence. (M-Q) Intensity analysis of (H-L). Magnification 100×, scale bar: 100 μm. Magnification 200×, scale bar: 50 μm. Data are expressed as the means ± standard deviation of 3 independent experiments.

TNFSF11, TNF ligand superfamily member 11; HDM, house dust mite; TNFRSF11A, TNF receptor superfamily 11A; IL, interleukin; EMBP, eosinophil major basic protein; GAPDH, glyceraldehyde 3-phosphate dehydrogenase; HE, hematoxylin–eosin; PAS, periodic acid–Schiff; TGFβ1, transforming growth factor β1; STAT3, signal transducer and activator of transcription 3; NS, not significant.

*P < 0.05, **P < 0.01, ***P < 0.001, ****P < 0.0001.

Provisional

Allergy, Asthma & Immunology Research AAIR

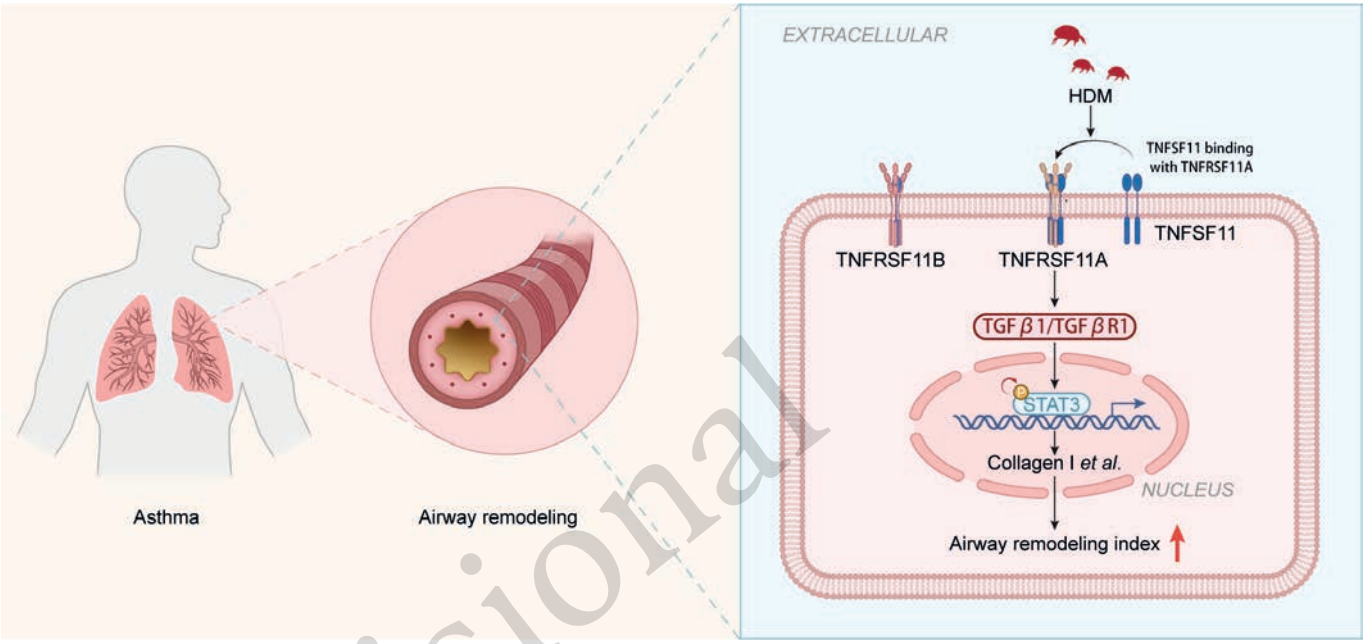

Fig. 11. Structure of TNFSF11/TNFRSF11A axis aggravated airway remodeling by strengthening TGFβ1/STAT3 signaling in HDM-induced asthma.
TNFSF11, TNF ligand superfamily member 11; TNFRSF11A, TNF receptor superfamily 11A; TNFRSF11B, TNF receptor superfamily 11B; TGFβ1, transforming growth factor β1; TGFβR1, transforming growth factor β receptor type 1; STAT3, signal transducer and activator of transcription 3; HDM, house dust mite.

Provisional

(PLC) can degrade occludin.[34] Downregulation of airway epithelial occludin increases asthma susceptibility and airway remodeling.[35,36] TNFSF11 regulates Src and PLC in human endothelial cells, and PLC regulates occludin expression through PKC phosphorylation.[34,37] Occludin plays an important role in the occurrence and development of asthma. This study showed that occludin expression significantly deceased in the TNFSF11-stimulated HBE cells (data not shown). In conclusion, TNFSF11-mediated occludin-dependent airway epithelial injury plays an important role in the occurrence and development of airway remodeling in asthma.

Mucus hypersecretion is one of the important characteristic pathological changes in patients with asthma. Approximately 20%–25% of the airway epithelium in a patient with asthma is composed of goblet cells; thus, mucus is excessively secreted.[38] This study showed that patients with asthma secreted more mucus than normal subjects (data not shown). PAS staining results in mice indicated that epithelial mucus secretion was upregulated after rmTNFSF11 protein stimulation (**Fig. 4C**). Weakened airway elasticity and excessive mucus secretion might block the airway lumen, making patients feel asphyxiated, and asphyxiation can occur in severe cases.[39] Mucus secretion is closely related to IL-17A and STAT3 phosphorylation.[40,41] mRNA transcriptome results indicated that the TNFSF11/TNFRSF11A axis might regulate IL-17A production in asthma (**Fig. 7A**). Therefore, we speculated that TNFSF11-induced mucous hypersecretion is a potential target for asthma treatment.

Canonical Th2 cytokines play an important role in the development and deterioration of asthma. IL-13 enhances the potency of histamine, aminophenol, and leukotriene D4 as systolic agonists, and IL-4 only increases the potency of histamine.[42] IL-5 does not induce hyperreactivity in isolated human small airways.[43] However, their roles in inflammation and airway remodeling are unaffected.[44,45] In addition, macrophages are innate immune cells with conflicting functional roles and involved in proinflammatory and anti-inflammatory processes; these functions have a profound impact on the pathogenesis of asthma.[46]

https://doi.org/10.4168/aair.2024.16.e33

Anti-inflammatory innate immune function is attributed to M2 macrophages, which are activated by factor, such as Th2 cytokines, including IL-4 and IL-13. This study showed that pretreatment with denosumab improved IL-4 level in HDM-induced HSC-NOG-EXL mice with HDM-induced asthma. In addition, TNFSF11 and Eos had a close correlation, indicated that TNFSF11 affects immune homeostasis in asthma.

Reconstructing humanized asthmatic mice are important to study asthma pathogenesis. A study reported on HDM-induced asthma in humanized NOD/SCID murine model.[16] HSC-NOG-EXL mice show a human immune system for the preclinical studies of asthma.[47-49] In our previous study, we constructed a humanized mouse model using human IL-33 to study airway remodeling and Muc-5ac secretion.[15] In the present study work, denosumab was verified to improve airway inflammation, remodeling, and mucus secretion through TGFβ1/STAT3 phosphorylation in HSC-NOG-EXL mice with asthma, laying a solid foundation for the clinical trial of monoclonal antibodies.

In summary, the inhibition of the TNFSF11/TNFRSF11A axis effectively improves airway remodeling in HDM-induced asthma. The inhibition of TNFSF11 by denosumab injection to cut off TNFSF11/TNFRSF11A axis signaling is a potential therapeutic strategy for asthma.

ACKNOWLEDGMENTS

This work was supported by the National Natural Science Foundation of China (Grant Nos. 82270032, 82100056), the Key Research and Development Program of Shandong Province (Grant No. 2021SFGC0504), Shandong Provincial Natural Science Foundation (Grant Nos. ZR2021LSW015, ZR2021QH170), and Jinan Clinical Medicine Research Program for Respiratory Disease (Grant No. 202132002). We are grateful to Professor Jie Dai at Shanghai Bioprofile Technology Company Ltd. for their assistance and suggestions.

SUPPLEMENTARY MATERIALS

Supplementary Table S1

Characteristics of the study human subjects

Supplementary Fig. S1

Gene identification report of *Tnfsf11*$^{+/-}$ and *Tnfrsf11a*$^{+/-}$ mice.

Supplementary Fig. S2

Flow cytometry results of humanized HSC-NOG-EXL mice.

REFERENCES

1. Zhan W, Luo W, Zhang Y, Xiang K, Chen X, Shen S, et al. Sputum transcriptomics reveals FCN1+ macrophage activation in mild eosinophilic asthma compared to non-asthmatic eosinophilic bronchitis. Allergy Asthma Immunol Res 2024;16:55-70. PUBMED | CROSSREF
2. Hoshino M, Akitsu K, Ohtawa J, Kubota K. Long-term efficacy of house dust mite sublingual immunotherapy on clinical and pulmonary function in patients with asthma and allergic rhinitis. J Allergy Clin Immunol Glob 2024;3:100206. PUBMED | CROSSREF

Provisional Provisional

3. Yao L, Yuan X, Fu H, Guo Q, Wu Y, Xuan S, et al. Epithelium-derived cystatin SN inhibits house dust mite protease activity in allergic asthma. Allergy 2023;78:1507-23. PUBMED | CROSSREF
4. Zhang D, Yang H, Dong XL, Zhang JT, Liu XF, Pan Y, et al. TL1A/DR3 axis, a key target of TNF-a, augments the epithelial-mesenchymal transformation of epithelial cells in OVA-induced asthma. Front Immunol 2022;13:854995. PUBMED | CROSSREF
5. Khosla S. Minireview: the OPG/RANKL/RANK system. Endocrinology 2001;142:5050-5. PUBMED | CROSSREF
6. Boyle WJ, Simonet WS, Lacey DL. Osteoclast differentiation and activation. Nature 2003;423:337-42. PUBMED | CROSSREF
7. Bonnet N, Bourgoin L, Biver E, Douni E, Ferrari S. RANKL inhibition improves muscle strength and insulin sensitivity and restores bone mass. J Clin Invest 2019;129:3214-23. PUBMED | CROSSREF
8. Xiong J, Le Y, Rao Y, Zhou L, Hu Y, Guo S, et al. RANKL mediates muscle atrophy and dysfunction in a cigarette smoke-induced model of chronic obstructive pulmonary disease. Am J Respir Cell Mol Biol 2021;64:617-28. PUBMED | CROSSREF
9. Gregorczyk I, Maślanka T. Blockade of RANKL/RANK and NF-κB signalling pathways as novel therapeutic strategies for allergic asthma: a comparative study in a mouse model of allergic airway inflammation. Eur J Pharmacol 2020;879:173129. PUBMED | CROSSREF
10. Gregorczyk I, Jasiecka-Mikołajczyk A, Maślanka T. Blockade of NF-κB translocation and of RANKL/RANK interaction decreases the frequency of Th2 and Th17 cells capable of IL-4 and IL-17 production, respectively, in a mouse model of allergic asthma. Molecules 2021;26:3117. PUBMED | CROSSREF
11. Yang X, Wang X, Chi M, Zhang M, Shan H, Zhang QH, et al. Osteoprotegerin mediate RANK/RANKL signaling inhibition eases asthma inflammatory reaction by affecting the survival and function of dendritic cells. Allergol Immunopathol (Madr) 2019;47:179-84. PUBMED | CROSSREF
12. Fu L, Zhao J, Huang J, Li N, Dong X, He Y, et al. A mitochondrial STAT3-methionine metabolism axis promotes ILC2-driven allergic lung inflammation. J Allergy Clin Immunol 2022;149:2091-104. PUBMED | CROSSREF
13. Reddel HK, Bacharier LB, Bateman ED, Brightling CE, Brusselle GG, Buhl R, et al. Global Initiative for Asthma Strategy 2021: executive summary and rationale for key changes. Eur Respir J 2021;59:2102730. PUBMED | CROSSREF
14. Zhang D, Xu C, Zhang J, Zeng R, Qi Q, Xu J, et al. Plasma TNFRSF11B as a new predictive inflammatory marker of sepsis-ARDS with endothelial dysfunction. J Proteome Res 2023;22:3640-51. PUBMED | CROSSREF
15. Zhang D, Zhang J, Xu C, Qi Q, Zeng R, Liu X, et al. A humanized mouse model to study asthmatic airway remodeling and Muc-5ac secretion via the human IL-33. Allergy 2024;79:1364-7. PUBMED | CROSSREF
16. Sun X, Hou T, Cheung E, Iu TN, Tam VW, Chu IM, et al. Anti-inflammatory mechanisms of the novel cytokine interleukin-38 in allergic asthma. Cell Mol Immunol 2020;17:631-46. PUBMED | CROSSREF
17. Qi Q, Xu J, Wang Y, Zhang J, Gao M, Li Y, et al. Decreased sphingosine due to down-regulation of acid ceramidase expression in airway of bronchiectasis patients: a potential contributor to pseudomonas aeruginosa infection. Infect Drug Resist 2023;16:2573-88. PUBMED | CROSSREF
18. Park JH, Jeong E, Lin J, Ko R, Kim JH, Yi S, et al. RACK1 interaction with c-Src is essential for osteoclast function. Exp Mol Med 2019;51:1-9. PUBMED | CROSSREF
19. Post S, Rozeveld D, Jonker MR, Bischoff R, van Oosterhout AJ, Heijink IH. ADAM10 mediates the house dust mite-induced release of chemokine ligand CCL20 by airway epithelium. Allergy 2015;70:1545-52. PUBMED | CROSSREF
20. He X, Wang L, Li H, Liu Y, Tong C, Xie C, et al. CSF2 upregulates CXCL3 expression in adipocytes to promote metastasis of breast cancer via the FAK signaling pathway. J Mol Cell Biol 2023;15:mjad025. PUBMED | CROSSREF
21. Lipworth B, Chan R, Kuo C. Systemic IL-6 and severe asthma. Am J Respir Crit Care Med 2020;202:1324-5. PUBMED | CROSSREF
22. Xu T, Wu Z, Yuan Q, Zhang X, Liu Y, Wu C, et al. Proline is increased in allergic asthma and promotes airway remodeling. JCI Insight 2023;8:e167395. PUBMED | CROSSREF
23. Li J, Sarosi I, Yan XQ, Morony S, Capparelli C, Tan HL, et al. RANK is the intrinsic hematopoietic cell surface receptor that controls osteoclastogenesis and regulation of bone mass and calcium metabolism. Proc Natl Acad Sci U S A 2000;97:1566-71. PUBMED | CROSSREF
24. Loser K, Mehling A, Loeser S, Apelt J, Kuhn A, Grabbe S, et al. Epidermal RANKL controls regulatory T-cell numbers via activation of dendritic cells. Nat Med 2006;12:1372-9. PUBMED | CROSSREF
25. Cremer I, Dieu-Nosjean MC, Maréchal S, Dezutter-Dambuyant C, Goddard S, Adams D, et al. Long-lived immature dendritic cells mediated by TRANCE-RANK interaction. Blood 2002;100:3646-55. PUBMED | CROSSREF

Provisional Provisional

26. Standl M. Limited side effects of asthma treatment on growth and bone health in children. Thorax 2022;77:741. PUBMED | CROSSREF
27. Meng L, Zhao P, Jiang Y, You J, Xu Z, Yu K, et al. Extracellular and intracellular effects of bioactive glass nanoparticles on osteogenic differentiation of bone marrow mesenchymal stem cells and bone regeneration in zebrafish osteoporosis model. Acta Biomater 2024;174:412-27. PUBMED | CROSSREF
28. Chalitsios CV, McKeever TM, Shaw DE. Incidence of osteoporosis and fragility fractures in asthma: a UK population-based matched cohort study. Eur Respir J 2021;57:2001251. PUBMED | CROSSREF
29. Chotiyarnwong P, McCloskey EV. Pathogenesis of glucocorticoid-induced osteoporosis and options for treatment. Nat Rev Endocrinol 2020;16:437-47. PUBMED | CROSSREF
30. Joulia R, Puttur F, Stölting H, Traves WJ, Entwistle LJ, Voitovich A, et al. Mast cell activation disrupts interactions between endothelial cells and pericytes during early life allergic asthma. J Clin Invest 2024;134:e173676. PUBMED | CROSSREF
31. Gregory LG, Lloyd CM. Orchestrating house dust mite-associated allergy in the lung. Trends Immunol 2011;32:402-11. PUBMED | CROSSREF
32. Doyle AD, Masuda MY, Pyon GC, Luo H, Putikova A, LeSuer WE, et al. Detergent exposure induces epithelial barrier dysfunction and eosinophilic inflammation in the esophagus. Allergy 2023;78:192-201. PUBMED | CROSSREF
33. Akdis CA. The epithelial barrier hypothesis proposes a comprehensive understanding of the origins of allergic and other chronic noncommunicable diseases. J Allergy Clin Immunol 2022;149:41-4. PUBMED | CROSSREF
34. Feldman GJ, Mullin JM, Ryan MP. Occludin: structure, function and regulation. Adv Drug Deliv Rev 2005;57:883-917. PUBMED | CROSSREF
35. Yuan L, Liu H, Du X, Yao Y, Qin L, Xia Z, et al. Airway epithelial ITGB4 deficiency induces airway remodeling in a mouse model. J Allergy Clin Immunol 2023;151:431-446.e16. PUBMED | CROSSREF
36. Steelant B, Farré R, Wawrzyniak P, Belmans J, Dekimpe E, Vanheel H, et al. Impaired barrier function in patients with house dust mite-induced allergic rhinitis is accompanied by decreased occludin and zonula occludens-1 expression. J Allergy Clin Immunol 2016;137:1043-1053.e5. PUBMED | CROSSREF
37. Kim YM, Kim YM, Lee YM, Kim HS, Kim JD, Choi Y, et al. TNF-related activation-induced cytokine (TRANCE) induces angiogenesis through the activation of Src and phospholipase C (PLC) in human endothelial cells. J Biol Chem 2002;277:6799-805. PUBMED | CROSSREF
38. Nomura N, Matsumoto H, Sunadome H, Oguma T, Hirai T. Importance of mucus burden and mucociliary impairment in asthma. J Allergy Clin Immunol 2023;151:1410-1. PUBMED | CROSSREF
39. Fahy JV, Dickey BF. Airway mucus function and dysfunction. N Engl J Med 2010;363:2233-47. PUBMED | CROSSREF
40. Quan J, Wen X, Su G, Zhong Y, Huang T, Xiong Z, et al. Epithelial SIRT6 governs IL-17A pathogenicity and drives allergic airway inflammation and remodeling. Nat Commun 2023;14:8525. PUBMED | CROSSREF
41. Jung MA, Song HK, Jo K, Lee A, Hwang YH, Ji KY, et al. Gleditsia sinensis Lam. aqueous extract attenuates nasal inflammation in allergic rhinitis by inhibiting MUC5AC production through suppression of the STAT3/STAT6 pathway. Biomed Pharmacother 2023;161:114482. PUBMED | CROSSREF
42. Miller RL, Grayson MH, Strothman K. Advances in asthma: new understandings of asthma's natural history, risk factors, underlying mechanisms, and clinical management. J Allergy Clin Immunol 2021;148:1430-41. PUBMED | CROSSREF
43. Manson ML, Säfholm J, James A, Johnsson AK, Bergman P, Al-Ameri M, et al. IL-13 and IL-4, but not IL-5 nor IL-17A, induce hyperresponsiveness in isolated human small airways. J Allergy Clin Immunol 2020;145:808-817.e2. PUBMED | CROSSREF
44. Xie Y, Abel PW, Casale TB, Tu Y. T_H17 cells and corticosteroid insensitivity in severe asthma. J Allergy Clin Immunol 2022;149:467-79. PUBMED | CROSSREF
45. O'Byrne PM, Inman MD, Parameswaran K. The trials and tribulations of IL-5, eosinophils, and allergic asthma. J Allergy Clin Immunol 2001;108:503-8. PUBMED | CROSSREF
46. Fricker M, Gibson PG. Macrophage dysfunction in the pathogenesis and treatment of asthma. Eur Respir J 2017;50:1700196. PUBMED | CROSSREF
47. Ito M, Hiramatsu H, Kobayashi K, Suzue K, Kawahata M, Hioki K, et al. NOD/SCID/γ_c^{null} mouse: an excellent recipient mouse model for engraftment of human cells. Blood 2002;100:3175-82. PUBMED | CROSSREF
48. Ito R, Maruoka S, Soda K, Katano I, Kawai K, Yagoto M, et al. A humanized mouse model to study asthmatic airway inflammation via the human IL-33/IL-13 axis. JCI Insight 2018;3:e121580. PUBMED | CROSSREF
49. Ito R, Takahashi T, Katano I, Kawai K, Kamisako T, Ogura T, et al. Establishment of a human allergy model using human IL-3/GM-CSF-transgenic NOG mice. J Immunol 2013;191:2890-9. PUBMED | CROSSREF

Provisional Provisional